
Karl Christian Lautenschläger

Wirelessly Networked Coordination of Section Control for Agricultural Machines

Undergraduate Thesis in Information Systems Engineering

18 May 2021

Please cite as:

Karl Christian Lautenschläger, "Wirelessly Networked Coordination of Section Control for Agricultural Machines," Undergraduate Thesis (Studienarbeit), Faculty of Computer Science, TU Dresden, Germany, May 2021.

Wirelessly Networked Coordination of Section Control for Agricultural Machines

Undergraduate Thesis in Information Systems Engineering

vorgelegt von

Karl Christian Lautenschläger

geb. am 29.06.1998
in Magdeburg

angefertigt an der

**Technischen Universität Dresden
Fakultät Informatik
Networked Systems Modeling**

Betreuer: **Christoph Sommer**
Gutachter: **Christoph Sommer**

Abgabe der Arbeit: **18. Mai 2021**

Erklärung

Ich versichere, dass ich die Arbeit ohne fremde Hilfe und ohne Benutzung anderer als der angegebenen Quellen angefertigt habe und dass die Arbeit in gleicher oder ähnlicher Form noch keiner anderen Prüfungsbehörde vorgelegen hat und von dieser als Teil einer Prüfungsleistung angenommen wurde.

Alle Ausführungen, die wörtlich oder sinngemäß übernommen wurden, sind als solche gekennzeichnet.

Declaration

I declare that the work is entirely my own and was produced with no assistance from third parties.

I certify that the work has not been submitted in the same or any similar form for assessment to any other examining body and all references, direct and indirect, are indicated as such and have been cited accordingly.



(Karl Christian Lautenschläger)

Dresden, 18 May 2021

Abstract

Automatic Section Control is a precision agriculture technology, which tracks applied areas as polygons per machine and then automatically turns off applying machine parts while the machine drives over these tracked areas.

To enable joint cultivation with multiple machines, I developed two concepts for Inter-Vehicular Communication (IVC) in the agricultural domain, which consist of wide area networks enabling machines to share their polygons. One is based on LTE-M, which enables multicast transmissions to other machines and client-server-communication to a central polygon tracking entity, the server. The other concept consists of a LoRa-based Peer-To-Peer network, where all applied polygons are broadcasted. I conducted field experiments to prove the feasibility of LoRa, that allowed a polygons to be sent reliably over a distance of up to 2.3 km. In two simulation I analysed the concepts. Both concepts represent feasible plans. The LoRa-based system is more independent from any additional infrastructure than the LTE-M based concept. Whereas an centralized server can reduce the needed network polygon exchange.

Kurzfassung

Automatische Teilbreitenabschaltung ist eine Technologie in der Landtechnik, bei der eine Maschine bearbeitete Flächen eines Feldes als Polygone abspeichert. Sobald die Maschine eine Fläche ein zweites Mal bearbeiten würde, kann die Maschine anhand der gespeicherten Daten automatisch die agierenden Geräte, z.B. Spritzdüsen einer Pflanzenschutzspritze, abschalten.

In dieser Studienarbeit entwickelte ich zwei Konzepte für Inter-Vehicular- Communication zwischen den Landmaschinen, die den Austausch der Polygone und damit die gemeinsame Bodenbearbeitung ermöglichen. In der ersten Lösung wird LTE-M genutzt, um Polygone an einen zentralen Server zu senden und über LTE-M Multicasts mit anderen Maschinen auf dem Feld zu teilen. Das zweite Konzept ist ein LoRa Peer-To-Peer Netzwerk, welchen über Broadcasts den Austausch der Polygone ermöglicht. In Feldmessungen konnte ich zeigen, dass LoRa eine geeignete Technologie ist, da ich Broadcasts der Polygone über 2.3 km zuverlässig empfangen konnte. In zwei Simulationen demonstrierte ich, dass LoRa eine ausreichende Datenrate hat, jedoch der zentrale Server der ersten Lösung den benötigten Austausch an Polygonen reduzieren kann.

Contents

| | |
|--|------------|
| Abstract | iii |
| Kurzfassung | iv |
| 1 Introduction | 1 |
| 2 Related Work | 3 |
| 3 Fundamentals | 5 |
| 3.1 IEEE 802.11p | 5 |
| 3.2 LTE-M | 6 |
| 3.3 LoRa | 8 |
| 3.4 Automatic Section Control Systems | 11 |
| 4 System design | 15 |
| 4.1 Requirements of the Agricultural Domain on IVC | 15 |
| 4.2 Application Data Structure | 17 |
| 4.3 LTE-M - based Client - Server Network | 18 |
| 4.4 LoRa - based P2P Network | 22 |
| 5 Evaluation | 28 |
| 5.1 LoRa test environment | 28 |
| 5.2 LoRa test results | 34 |
| 5.3 Simulation studies | 37 |
| 5.4 Comparison of the MVSC systems | 43 |
| 6 Conclusion | 47 |
| Bibliography | 54 |

Chapter 1

Introduction

In large-scale agricultural farming, several operations must sometimes be carried out by multiple machines simultaneously due to restrictions imposed by short time windows. These can be found by operating on so-called "Minutenböden". The term defines soils with very high clay contents, which can only be cultivated for a very short time. The name itself is an exaggeration and suggests that one is only able to work on that ground for a few minutes while, in reality, work can be carried out over time periods of a few hours.

A solution for operating in short time windows is the usage of multiple machines for joint cultivation. One problem regarding this is the over-application of crops, that tends to occur. Due to the large working areas of the machines, for example sprayers, it is very likely that parts of the machine drive over an already applied area and in doing so treat this area a second time. This can affect plant growth and therefore the yield. Additionally, it causes extra costs by buying additional spraying liquid.

Without a coordinating system the joint cultivation could fail.

Therefore modern agricultural machines are equipped with an Automatic Section Control (ASC) system for processes like planting, fertilizing or spraying. The machine must be able to control separate applying sections. In this thesis I use the phrase applying sections as a generalisation of Machine parts, that are separate controllable section that carry out the operation of the machine. A sprayer, for example, can have individual boom section valves or individual nozzle valves, which I generally define as applying sections. During these operations the ASC system maps the applied area in polygons. This segmentation can be generated by knowing the positional coordinates from a GPS receiver and the machinery geometry. Knowing the covered area, the agricultural sprayer, for example, can automatically turn off the separate applying sections while driving over already treated areas. As soon as its boom sections enter an untreated area, the system turns on the sections.

So far ASC is not applicable for joint cultivation, because every machine would only

keep track of their own covered field and therefore still work in an area, where other machines already completed the same job. A solutions could be assigning an area to every machine as is proposed in [1]. This way every sprayer or planter would probably only treat the ground twice near the border of its assigned sector. But it is pointed out by [1], that since each machine can differ in tank capacity, operating width, operating speed and turning radius and each field can have varying obstacles in shape and size, such modeling can be very difficult.

Therefore another solution is needed, which is somehow independent of the mentioned variables. It could be a system to exchange treated areas as polygons between machines. As soon as all vehicles are able to identify the already applied areas, they can carry out the same operation in the field using ASC.

In order to implement a wireless networked coordination of ASC across multiple agricultural machines, I develop and compared two Multi Vehicles Section Control (MVSC) system concepts. Thereby I plan, that each concept is able to operate up to ten machines in up to three groups over a field of up to 300 ha. The number of groups is derived from the number of possible activities: planting, spraying and fertilising. Above this, the fields can have any shapes with a maximum field diameter of up to 3 km long. Each concept enables the machines to share polygons over long ranges with one another. This allows the ASC system of each machine to work on the basis of the known shared polygons. This approach can reduce the over-applying crop inputs, while spraying, planting or fertilizing is carried out by multiple machines simultaneously.

The proposed MVSC systems implement Inter-Vehicular Communication (IVC) on the basis of the Low Power Wide Area Networking (LPWAN) technologies LTE-M and LoRa. The last mentioned is used for setting up a Peer-To-Peer Network (P2P network) among all operating units, which allows polygons being broadcasted and thereby made available for all machines. LTE-M enables client-server-communications, where a centralized server tracks all applied areas as polygons and distributes them to all machines and polygons can be shared as multicasts.

Chapter 2

Related Work

An MVSC system can be regarded as a use case for IVC in agricultural environments, which has similar requirements to some solutions of Precision Farming or Smart Farming.

The technology used for the IVC in agricultural domains has to enable reliable networking with a good coverage in a large area. Due to the different possible terrains with small woods or hills, the Line-Of-Sight (LoS) cannot be guaranteed for every communication.

Similar requirements are pointed out for an Intelligent Farming solution developed by Nóbrega et al. [2]. The authors state, that the system needs to be able to reliably communicate over a large area. Thereby different obstacles can occur. Additionally, the authors mention that their devices have to be small and light and are battery-powered. In their work they analysed possible technologies and protocols which can enable a system to track the movement of sheep with regards to the mentioned requirements.

Besides livestock tracking, concepts of sensor networks are often presented as precision agriculture solutions. Islam et al. [3] review applications and communication technologies for Internet of Things and unmanned aerial vehicles for smart farming and smart housing purposes. In two case studies LoRaWAN and satellite communication systems are evaluated. However, this work focuses more on long range communication technologies in context of sensor networks than on IVC in the agricultural domain.

Another precision farming system which includes a sensor network to measure soil moisture, humidity and temperature among other values is designed by Wu et al. [4].

But precision farming use cases differ in the devices. As Devices are mounted to machines and powered by them, they don't have to be small and their power consumption is not limited by a battery. Klingler, Blobel, and Dressler [5] suggest

developing IVC for agricultural environments on basis of IEEE 802.11p and also conducted field measurements to test feasibility of such network in the agricultural context. The authors mention, that they don't know of any prior work investigating the usage of IEEE 802.11p in agricultural domains.

To the best of my knowledge, the only other work on coordinating multiple agricultural machines simultaneously is from Ali et al. [6]. They developed a system, which can guide a tractor with trailers to a harvester so that the harvester can empty its corn tank into the tractor's trailers. They equipped the machines with a cellular network technology to send position data, located via Global Positioning System (GPS), as a General Packet Radio Service to a central server. The server uses the location information to provide guidance instructions for the machines.

Chapter 3

Fundamentals

3.1 IEEE 802.11p

IEEE 802.11p is a modification of the IEEE 802.11 standard to enable inter-vehicle communication [7]. It uses the 5.9 GHz frequency spectrum for Intelligent Transport Systems [8], [5]. IEEE 802.11p is intended to provide robust connections together with fast setup for moving vehicles [7].

The Wireless Access in Vehicular Environments (WAVE) operating mode and the WAVE Basic Service Set are implemented by the IEEE 802.11p Media Access Control (MAC) layer to fulfill the requirements of vehicular usage [9]. The following explanations of both amendments are mentioned in the same paper. The WAVE mode enables stations to send and receive data using a wildcard Basic Service Set identification at any time without having joined a Basic Service Set. This decreases the overhead for setting up a connection. WAVE Basic Service Set enables private services in dedicated short-range communications. The initiating station shares WAVE Advertisement messages, which allow other stations to join to WAVE Basic Service Set.

A feasibility study on IEEE 802.11p for agricultural use cases was conducted by Klingler, Blobel, and Dressler [5]. In the described experiments the received signal strength, delay and goodput were investigated. For this purpose, a receiver was mounted on top of the driver cabin of a harvester and a sender was placed on the roof of a tractor. In the first experiment the receiver drove down a straight road away from the sender, which was at a fixed position. After 1700 m no packets were received anymore, because LoS was lost due to a slight turn of the road. Another of their experiments revealed that the size of harvesting machines and their additional mechanics can effect the signal propagation and thereby have an impact in the received signal strength. The authors state that this occurs because the additional

mechanics can limit the LoS.

3.2 LTE-M

LTE-M is an abbreviation for LTE-Machine-Type-Communication, which is a technology for LPWAN defined as a 3GPP standard first published in Release 13 specification [10]. The intention was to provide a cellular Machine-To-Machine (M2M) connection with a low uplink latency and a better network coverage for very high number of devices which should be available for a low price and able to last long on battery [11].

It uses the licensed spectrum [12]. LTE-M is a cellular network technology operating on available Long-Term Evolution (LTE) infrastructure made available by software updates from the Mobile Network Operator (MNO) [12].

Sommer and Dressler [8] explain that cellular networks contain base stations distributed in a large area of land. An authorized end device in the area around each station, named cell, can connect to the base station and is served by it. As soon as the device moves to another cell, it switches to the corresponding station.

A white paper [12] states that LTE-M has the following characteristics: It offers half and full duplex connections, which can have a peak data rate of 1 Mbit/s on downlink on a Bandwidth (BW) of 1.4 MHz. The maximum Coupling Loss can be up to 156 dB. Liberg et al. [13] explain the maximum Coupling loss as the maximum loss in the conducted power level, which allows a system to still deliver its services.

Liberg et al. [13] also mention the following data rates ranging from 0.8 kbit/s ... 1000 kbit/s for a LTE-M operating on half duplex mode with the sending power of 23 dBm (200 mW). They say, that 0.8 kbit/s can be achieved on a maximum Coupling Loss of 164 dB. It can rise to 40.1 kbit/s on a Coupling Loss of 144 dB until a maximum data rate of 1 Mbit/s available as an instantaneous peak.

LTE-M operates in the system bandwidths 1.4 MHz, 3 MHz, 5 MHz, 10 MHz, 15 MHz or 20 MHz which are equal to the ones used by LTE [13]. LTE downlink and uplink resources can be dynamically allocated for LTE traffic and LTE-M traffic [13]. Using multimode radio modules for LTE-M additionally enables users to employ other bearers, for example 2G or 3G [12].

Dawaliby, Bradai, and Pousset [14] simulated the performance of LTE-M and LTE Category 0 for M2M communication and compared them. LTE Category 0 is explained by the authors as new user equipment which is optimized towards M2M communication. They say, that it can provide lower data rates, less power consumption and suitable delays for transmissions. The simulation results for LTE-M indicated a wider range as LTE Category 0 and a suitable throughput. Additional a larger

number of machines were able to connect to the LTE-M network. At a distance of 20 km between the LTE-M device and the LTE base station, the simulation resulted in a throughput of over 0.75 Mbit/s, a Packet Reception Ratio (PRR) of over 75 % and a delay of less than 125 ms.

Liberg et al. [13] mention, that LTE-M offers various Coverage Enhancement (CE) techniques to improve network coverage in expected difficult coverage conditions. The authors state, that these techniques include the two modes A and B which are based on repeating of physical signals and channels. Furthermore they explain that mode A provides a small amount of repetitions to compensate the worse capability of low-cost devices and that mode B provides a huge amount of repetition to optimize coverage in all needed situations.

Experiments to test the LTE-M coverage were conducted in Denmark [11]. It was found out that using LTE-M 80 % of the deep indoor users, which had an average maximum Coupling Loss of 145 dB inside buildings, can be served. The results also pointed out a 99.9 % outdoor coverage.

Liberg et al. [13] state that 3GPP Release 14 introduced multicast transmissions which are Single-Cell Point-to-Multipoint transmissions operable only in idle mode. The authors mention, that a Single Cell Multicast Traffic Channel with a maximum channel bandwidth of either 1.4 MHz or 5 MHz on a maximum transport block size of 1000 bit and 4008 bit per multicast service can be configured. They explain, that a transport block defines the data structure of the physical layer. Every data from a higher layer needs to be fitted into this transport blocks. The authors also define the idle mode. In this mode the initial cell selection, the cell reselection and the paging procedures are carried out. Paging is explained by the authors as an occasional opportunity of the network to contact the LTE-M device. The authors furthermore state, that this multicast feature is based on a Single-Cell Point-to-Multipoint feature for LTE devices.

Group communication services for cellular networks including LTE are described in [15]. It is a technical specification, which defines multipoint services as a opportunity to share the same data with multiple LTE-M devices. It further explains, that groups can be set up, where members can be authorized to use multipoint services within the group. These members are call Transmitter Group Member.

[10] additionally provides the information, that up to 128 Single Cell Multicast Traffic Channel can be set up per cell. Such a channel can offer a data rates of up to 1 Mbit/s or up to 4 Mbit/s at the channel bandwidth of 1.4 MHz or 5 MHz respectively.

Future-proof Internet-of-Things technologies for smart agriculture are discussed in [3], where LTE-M is mentioned as an option for massive Machine-type communications. Liberg et al. [13] explain massive Machine-Type-Communications as a specification, where a many sensor devices must be able to send their small amount

of data. In contrast to critical Machine-Type Communications their communications are not delay sensitive. It is defined in [16] that a required network capacity of 1 000 000 devices per km² to fulfill the requirements of massive Machine-type Communications. In this regard [13] remarks, that the outage, which indicates the percentage of devices not served by the network, would exceed 1 % for this mentioned system load and at least 3 or more narrowbands are needed in a cell. [13] additionally states that 361 000 devices per km² can operate in LTE-M per narrowband with an outage of below 1 %. A so-called narrowband is defined in [13] as resource for the physical channels and signals of LTE-M. It is further explained that each uses six Physical Resource Blocks, where each has a bandwidth of 180 kHz

3.3 LoRa

LoRa is an abbreviation for long range. It refers to a LPWAN protocol invented by Cycleo and bought by Semtech in 2012 [17]. LoRa specifies a physical layer implementation [18].

It operates in unlicensed sub-gigahertz radio frequency bands [19]. These are 868 MHz in Europe , 915 MHz in America and 433 MHz in Asia [18]. The usage of these frequencies is regulated by each country. The current frequency plan for Germany can be found at the german Federal Network Agency as "Funkanwendungen mit geringer Reichweite; Non-specific Short Range Devices (SRD)" [20].

For every frequency range the document specifies a maximum Equivalent Radiated Power (ERP) and sometimes a duty cycle limitation or techniques for frequency access and interference reduction whose performance level is at least equal to the essential requirements Directive 2014/53/EU of the European parliament and of the council. The duty cycle, indicating the fraction of time a resource is used for sending, varies in the mentioned regulation from 0.1 % to 10 %.

LoRa can be parameterised to meet the requirements of the different work scenarios. Bertoldo et al. [17] mention the following parameters and their explanations. These are the bandwidth, the Coding Rate (CR) and the Spreading Factor (SF). The bandwidth can either be 125 kHz, 250 kHz or 500 kHz and indicates the width of the signal. The CR, ranging from 4/5 to 4/8, defines the ratio of non-redundant sent bits. The SF ranges 6 to 12 and specifies the amount of bits needed for encoding each symbol. Shanmuga Sundaram, Du, and Zhao [19] further explain that a packet sent using a higher SF will be more resilient to any noise, but will also take more time on air and therefore result in a lower data rate . Additional the authors state that operating on a higher SF will also increase the possible communication range. Another parameter, the Transmission Power (TX power), is defined in the paper of Shanmuga Sundaram, Du, and Zhao [19]. The authors mention, that using a

higher TX power increases the received signal strength and therefore improves the resilience against possible path losses.

The LoRa data rate [21] is shown in Equation (3.1) depending on the SF, CR and the BW in Hz:

$$\text{Data Rate} = \text{SF} * \text{CR} * \frac{\text{BW}}{2^{\text{SF}}} \quad (3.1)$$

LoRa uses Chirp Spread Spectrum (CSS) modulation [22]. According to Shanmuga Sundaram, Du, and Zhao [19] chirps are information encoded in frequency varying linearly with time within a predefined bandwidth. They explain, that the frequency of pulses decreases or increases based on the encoded informations over a specific amount of time. The effect of CSS is explained in [17]. The authors explain that using this modulation technique results in a robustness against noise and multi-path fading and the Doppler effect.

An experiment studying the effect of the Doppler Shift on mobile LoRa applications is described in [22]. The results clearly show that over 85 % of the packets were received at a speed ranging from 50 km/h ... 80 km/h (13.89 m/s ... 22.23 m/s). The conducted analysis and measurements concluded a decreasing impact of the Doppler effect, while using a lower SF such as 7.

The LoRa frame structure starts with a preamble, which contains between 6 and 65 535 symbols [22]. The default preamble length is 8 symbols [23], where a symbol transmission time can be calculated [21], [22]:

$$\text{TimeSymbol} = \frac{2^{\text{SF}}}{\text{BW}} \quad (3.2)$$

This is followed by a mandatory preamble [22], which is 4.25 symbols long. It contains 2 frame synchronization symbols and 2 frequency synchronization symbols and a conjugate chirp which has the duration of a quarter of the symbol transmission time [24]. Xhonneux, Bol, and Louveaux [25] state that these synchronization symbols are called *sync words* and represent network identifier to enable differentiation between multiple LoRa networks operating on the same frequency.

The next part of the LoRa frame is a optional header, which can contain up to 3 Byte [22], where 1 Byte is the header checksum [24]. The header is encoded with a CR of 4/8 and contains the payload length, information about the used data rate and a bit, which indicates a Cyclic Redundancy Check (CRC) of the payload [24]. When the optional header is disabled, the receiving nodes must set the parameters CRC and CRC presence bit beforehand [24]. The maximum payload in the LoRa frame structure is 255 Byte [22]. LoRa modulation supports CRC, which extends the packet structure for up to 2 Byte at the end of the frame structure on uplink transmissions [22].

Having LoS communication established, LoRa-based networks can have long communication ranges. The results of measurements described in [26] state that a PRR of over 80 % was achieved on land on distances up to 5 km. The ratio decreased to 60 % at distances between 5 km ... 10 km and 10 km. On water, the PRR was 62 % with a communication range varying from 15 km ... 30 km.

The Fresnel zone is a cylindrical ellipse between a transmitter and a receiver node [21]. The scheme of a Fresnel Zone is shown in Figure 3.1. Jebril et al. [21] state that if over 40 % of the Fresnel Zone are not free of obstructions, such as buildings, mountains, or trees, signal energy losses can incur. Aref and Sikora [27] present a formula for calculating the radius of the first Fresnel Zone, which is shown in Equation (3.3). The variable d_1 represents the distance to the sender. d_2 equals to the distance to the receiver. The LoRa wavelength is represented by λ .

$$R = \sqrt{\frac{\lambda * d_1 * d_2}{d_1 + d_2}} \quad (3.3)$$

As LoRa only specifies a physical layer implementation, it has no MAC layer implementation. But with an increasing density of LoRa devices, a larger number of nodes must share the medium in the same local geographical area. There are multiple techniques available to create non-interfering communication channels.

By using Frequency-Division Multiple Access (FDMA) different channels can be allocated on different frequency band spectres [8]. The open-source LoRaWAN specification builds MAC, network and application layer on top of LoRa [17]. Its protocol operates on three main channels with center frequencies at 868.10 MHz, 868.30 MHz and 868.50 MHz [28].

Like in other wireless technologies, it is also possible to set up multiple channels with Time-division Multiple Access (TDMA)[28]. Sommer and Dressler [8] explain that the scheme subdivides the media access time in equal-sized slots which can be assigned to different LoRa nodes. Furthermore the authors state that it has some

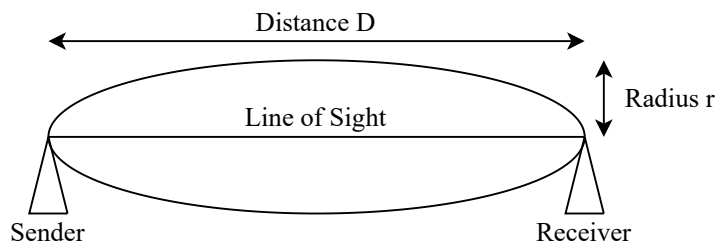


Figure 3.1 – Fresnel zone, which can be described as a cylindrical ellipse between sender and receiver devices

overhead in order to maintain tight time synchronizations among all nodes. Another doable technique is Code-Division Multiple Access (CDMA) [28]. Sommer and Dressler [8] mention that it is based on orthogonal spreading codes, multiplied by the data bits to be sent, which are assigned to different channels. They explain that the transmitted mixed signal is multiplied with the assigned channel spreading code and summed up for the duration of a bit at the receiving node. Furthermore the authors state that the receiver would be able to get its fraction of the original data under ideal conditions. As the SF are orthogonal, they can be used as different codes [28].

Ji and Yang [29] mention that there are not many owned and protected copyright restrictions for LoRa. For this reason, the authors further explain, the LoRa industry can offer modules for prices between 7\$ and 10\$. This enables autonomous network set-up at low cost.

3.4 Automatic Section Control Systems

ASC, also short referred to as Section Control, is a precision farming technology. The concept of ASC and its potential profit is described by Luck, Stombaugh, and Shearer [30]. The authors state, that ASC systems focus on reducing over-application of crop inputs. Therefore the machines are equipped with controllable applying sections which can be automatically switched off while passing over previously treated areas. Additionally, the machines can control the application flow of the sections and thereby maintain different precalculated application rates. The authors analysed the potential savings achieved through using ASC and were able to demonstrate significant reductions in over-application.

For analyzing current ASC systems the company the software *LACOS Computerservice GmbH*¹ provided to me their current ASC system software *LC:NAVGUIDE*, which is shown in Figure 3.2.

LC:NAVGUIDE uses the approach of tracking the applied areas by generating so-called multipolygons. Every generated multipolygon consists of a workarea-id, a list of polygons, as well as a starting timestamp and a finishing timestamp. Usually they only contain one polygon, which has usually no interiors. This data format is necessary in order to satisfy demands of different system states. A state where both outer boom sections are turned on and therefore operates on two separate areas, needs to be able to track and store two polygons simultaneously.

A multipolygon can meet these requirements. For easier sharing workareas via the LoRa P2P network, every multipolygon is splitted into its polygons. Every polygon gets its own identification.

¹<https://www.lacos.de>

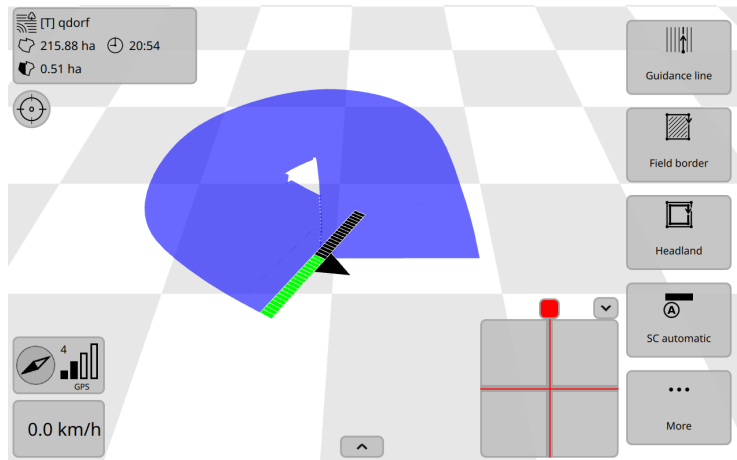


Figure 3.2 – Screenshot LC:NAVGUIDE / A simulated tractor turns of boom sections, while passing an already treated area.

The coordinates of every polygon are in the World Geodetic System from 1984 (WGS-84)-format and therefore contain longitude and latitude. To maintain a precision of at least 1.2 cm it is necessary to store the coordinates with at least seven decimal places.

In order to analyze the polygon creation frequency and the number of vertices in a polygon I used *LC:NAVGUIDE* to simulate a sprayer with a span of 36 m operating on a real field shape with a speed of 12 km/h (3.3 m/s), where every generated multipolygon is tracked together with a starting timestamp and a finishing timestamp. The shape of the simulation field, shown in Figure 3.3, is from a 210 ha area near Fraßdorf ($51^{\circ}43'40.4004''N$, $12^{\circ}6'43.272''E$) in Germany.

LACOS Computerservice GmbH additionally provided me with a GPS trace of a real sprayer with a span of 36 m operating on the mentioned field. I used the GPS trace as a path for the simulated sprayer. The generated polygons are visible in the Figure 3.3.

Analysing the simulation data, the following statistics become apparent. The ASC systems generated 582 polygons in a total time of 7 h and 35 min. The different workareas have various sizes and shapes. The average polygon covers an area of 0.37 ha. Especially in the corners there are many small polygons. Most of the workareas are rectangular. The polygons contain a minimum of 5 and a maximum of 74 coordinates. The exact distribution of coordinates per polygon is shown in Figure 3.4. A lot of polygons contain either around 5 coordinates or 30 coordinates. They can be generated in intervals between 1 s ... 74 s, as it is shown in Figure 3.5. The distribution shows a maximum at around 2 s and at around 55 s. Polygons are formed quickly when the machine is driving tight curves. Many of the polygons are rectangular with a maximum length of about 150 m and a width of 36 m, which is equivalent to the span of the sprayer. The ASC system allows this maximum length.

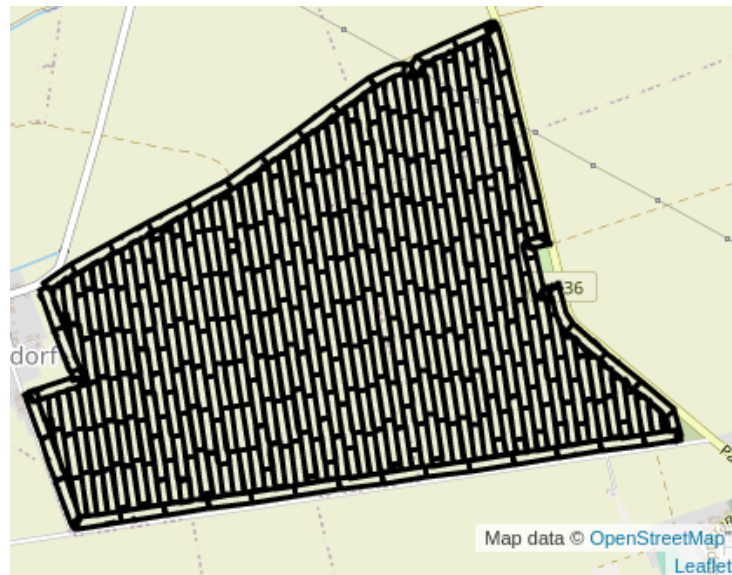


Figure 3.3 – OpenStreetMap, which represents the multipolygon coverage of a single sprayer with a span of 36 m operating on a 210 ha - field. Base map and data from OpenStreetMap and OpenStreetMap Foundation

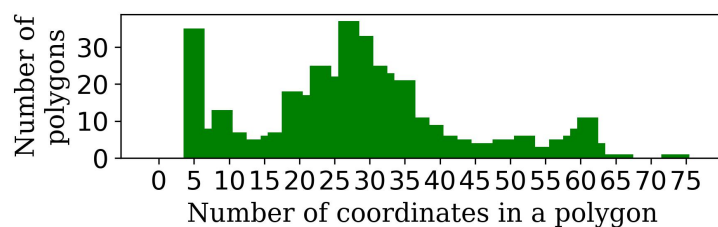


Figure 3.4 – Distribution of number of coordinates per polygon on the simulated field

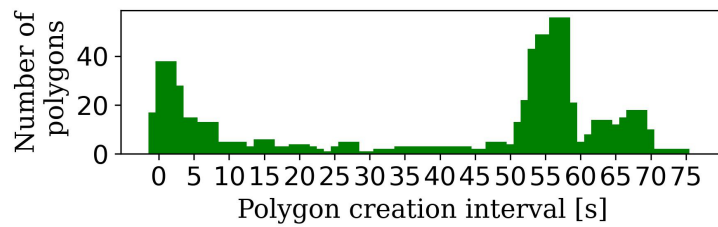


Figure 3.5 – Distribution of the polygon creation time on the simulated field

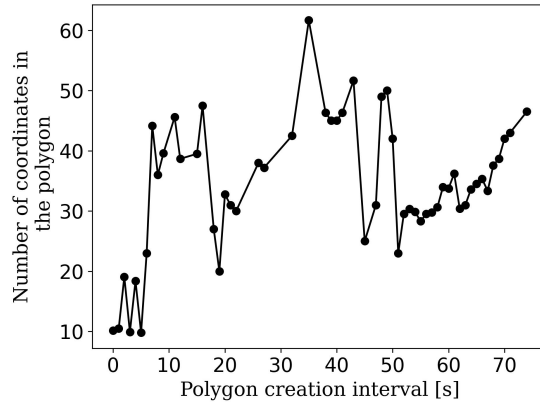


Figure 3.6 – Average number of coordinates in polygons in regards to the creation interval of the polygons on the simulated field

The operating sprayer needs about 55 s to travel this distance of 150 m. This results in the second maximum at 55 s visible in the mentioned distribution.

Figure 3.6 shows the average number of coordinates in a polygon in regards to the polygon creation time interval. It indicates that even polygons with a short creation interval can contain also a large number of coordinates. In general the designed systems need to be able to share all large number of coordinates at any time.

This knowledge of the data generated by an ASC system enables me to estimate requirements for the design of the MVSC systems. Looking at the maxima of polygon production time Figure 3.5, it is apparent, that MVSC systems must be able to share polygons in short time intervals. It is also recognizable, that their can be longer time intervals until new polygons are generated by the ASC systems.

Chapter 4

System design

4.1 Requirements of the Agricultural Domain on IVC

Having explained fundamental knowledge for this work, I attempt to describe to the best of my knowledge the possible problems and requirements for setting up IVC networks for the agricultural domain now.

Such a network can enable various joint cultivation and harvesting operations. Therefore it must be able to adopt to all different agricultural terrains. These can be field in a flat countryside and in a hilly terrain as agriculture is also practiced in low mountain ranges. To make joint cultivation worthwhile, the field cannot be too small. This implies that the technology being used for the network must be able to establish long range communications and should have a good and reliable coverage. Every field can have so-called islands. These can be woods, farm buildings, antenna towers or transmission towers in the field. Fields can also have various shapes with different indentations, where trees can grow or houses are built. A sample shape, which has various indentations with growing woods, is visible in Figure 4.1. This may result in two vehicles on a field having to communicate with one another without a line of sight.

Nóbrega et al. [2] generally state these requirements too. The authors analyzed different Internet of Things options for tracking the location of sheep. They state, among other requirements for their system, that they expect different obstacles and they regard the area to be covered as large.

Regarding the system's latency, the agricultural vehicle speed and the distance between machines have to be taken into account. Big agricultural machinery can be very long or wide. A sprayer for big machinery can easily have a span of 36 m. To prevent operating units from crashing into each other or getting jammed up together, they keep a wide safety space between them. While working on a field, they usually don't operate faster than 20 km/h (5.6 m/s). The company Väderstad is known for



Figure 4.1 – OpenStreetMap, showing a field shape with various indentations, where forests grow. Base map and data from OpenStreetMap and OpenStreetMap Foundation

their fast planters. On its website *Väderstad* mentions that one of their machines, the *Väderstad Tempo*, set a new world record for planting 502.05 ha with high precision and a speed over 20 km/s (5.6 m/s) within 24 hours². Therefore the latency for the use case of a MVSC system can be up to a few seconds. A working unit only has to know an area, newly treated by another machine, when it arrives at this position. Thereby at least the safety distance has to be covered with the low working speed, which takes a machine up to a few seconds.

All possible underlying long range technologies for this system have to offer a sufficient data rate for the different use cases.

²<https://www.vaderstad.com/en/planting/tempo-planter/the-world-record-planter/>

4.2 Application Data Structure

After explaining potential problems and requirements regarding implementing IVC for the MVSC system, I describe the development of the two concepts of the MVSC system. For both concepts a general application data structure is needed to enable sharing polygons among machines.

Every machine operating on a field gets a Machine Identifier (MI), a Process Identifier (PI) and up to two Group Identifiers (GIs) assigned by the MVSC system. The possible GIs are shown in Table 4.1. A single machine can be attributed with two GIs, when it carries out two operations simultaneously. An example of this is combined seeding and fertilising using the Doubleshot technique, where solid fertilizer and seeds are laid next to each other at the same time. I do not know of machines that carry out all three operations concurrently, therefore I set the limit of two GIs per machine. The MI ranges from 1 to 10 and identifies the machine on a field. The PI is a unique identifier to associate work within the specified field. All machines operating on this field use this PI for their communication. As soon as a machine receives data, containing a different PI, it can discard this data as it must be from another MVSC system operating on a neighbouring area.

A treated polygon in a MVSC system is tracked using the MI, the GIs, the PI and the polygon identifier, which can be a continuously counter per machine. The GIs define the operations carried out on the area, which can be precisely mapped by the polygon identifier, the MI and the PI to an area of a certain field.

Therefore the general application data structure shown in Figure 4.2 is developed. First the PI is encoded in 4 Byte. Only 4 Byte are chosen to make each packet very small to reduce the transmitting time.

The header contains this PI and additional 3 Byte resulting in a total size of 7 Byte.

| GIs | Operation |
|-----|-------------|
| 1 | planting |
| 2 | spraying |
| 3 | fertilizing |

Table 4.1 – Representation of group identifiers

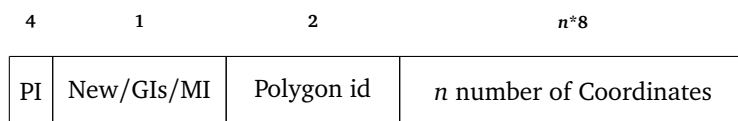


Figure 4.2 – Application data structure in Byte to encode and identify polygons in a MVSC system

| | | | | |
|-----|------|------|------|----|
| NEW | GI 1 | GI 2 | GI 3 | MI |
|-----|------|------|------|----|

Figure 4.3 – 1 Byte where the first 4 bit are used as flags and indicating a new polygon and the participating groups and the last 4 bit encode the MI

MI,GIs and a flag indicating a new polygon are encoded in 1 Byte. This is shown in Figure 4.3. If the sent data contains a new generated polygon the first bit is set. The following 3 bits are flags indicating whether a machine is part of group 1, group 2 or group 3. The last 4 bits represent the MI, ranging from 1 to 10, binary encoded. 11011010 for example indicates a packet from Machine 10, which is part of planting and fertilizing group and transmittes a new polygon.

The next 2 Byte contain a integer which encodes the polygon identifier. A 12 would represent the polygon identifier 12. Since each machine simply increments the polygon identifier for each new polygon, this polygon is also the twelfth of the machine.

After the header the coordinates are sent. Each contains a latitude value and a longitude value. Normally longitude and latitude are decimal numbers, which can be processed as 8 Byte double values. Multiplying them with 10^7 , they can be transmitted and stored as 4 Byte integers and thereby consume less space and still maintain a high resolution of 1.1 cm.

After explaining a potential solution for the application data structure, both concepts are presented in detail.

4.3 LTE-M - based Client - Server Network

A possible solution for developing a MVSC system is based on the underlying LPWAN technology LTE-M. Every operating machine is a client to a centralized server. The server application can be hosted for example on the farm's management computer and is accessible via internet. Every vehicle has to be able to establish a cellular network connection. The technology provides an easy way to communicate with a centralized server over the internet. For this purpose, the machines are equipped with a LTE-M modem and a sim-card. Various cellular standards are suitable for this use case. Since LTE-M offers an appropriate data rate of up to 1 Mbit/s with a full duplex connection and since it is also designed for long range M2M connections, it can be regarded as the most applicable standard.

The communication logic, which is described below, is illustrated as a sequence diagram in Figure 4.5.

Before starting any field operation the driving person specifies his name, the machine's name and whether he or she is going to spray, plant or fertilize. The application sends the data to the server and gets a MI, a PI and up to two GIs as response

While operating on the field, the ASC system on board of each machine tracks the applied area as multipolygons. For every polygon in a retrieved multipolygon, the client application updates the server by sending the polygon in the described data structure and additionally the current speed, position and direction of movement via the cellular connection. Then an array of coordinates, the coordinates of the center and the ids are stored for each received polygon. As a consequence of this process, every applied area of this field is known to the server. As it knows all MI and their assigned GIs, the server can also identify which operation was carried out on the stored polygons. A farm management software could use this data to visualize and track the work progress.

After receiving a client update, the server logic attempts to figure out in which area the machine could be working until it sends updates again. Using a field planner setting up paths for each operating vehicle, the server can easily estimate, where the vehicle is heading to. Without paths being planned, the potential working area can be calculated from the transmitted current position and the maximum working speed. A pessimistic approach must be used for calculating the potential working area, as it is not known, where the machine is navigated by the driver.

A circular area around the machine, shown in Figure 4.4, is calculated by multiplying the usual maximum working speed with a time of 30 s. This represents the potential working area. As a polygon creation interval can be up to 74 s, the client would have to send the position, speed and MI again after 30 s in order to enable the server to exchange needed polygons, which is described in the next paragraph. A time of 30 s is a trade off for a small potential working area versus the server load.

The server responds to the update request sent by the client by transmitting the polygon identifier and the corresponding MI of each polygon, whose calculated polygon center is included in the computed circle and which MI is not equal to the clients MI and where any GIs match any clients GIs. As these polygons are located in the possible working area of the machine and are already treated by another machine operating in the same group, there is a risk that the machine will treat them a second time.

However, these polygons can be known to the machine, because it has received the polygon via multicast transmissions, which is described in the next paragraph, and stored the polygon with its polygon id and the corresponding MI. In ideal circumstances every mentioned work area is available to the client by the multicast transmissions.

When a polygon id and the corresponding MI are unknown to the client, because of a failed transmission, the client requests the coordinates of this polygon from the server. As the server can provide all coordinates for any applied area, it can be regarded as a full backup for any failed or unsuccessful multicast transmission.

Using the described communications above, the machine ought to be aware of any

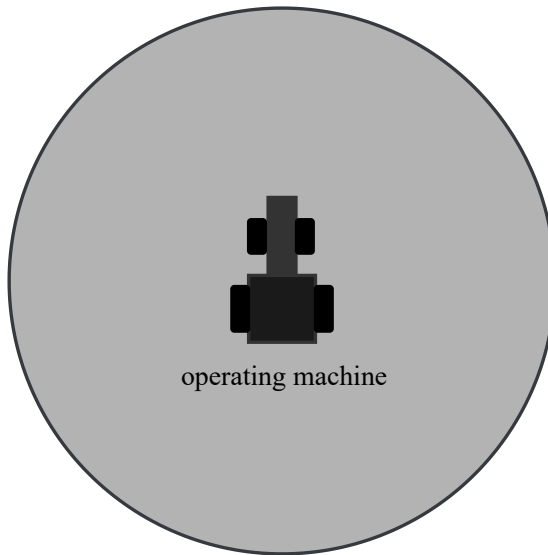


Figure 4.4 – Motion window until next position update depending on position and a positive maximum speed

already treated polygon in the area where it soon will operate. This is important as it enables its ASC system to exclude these areas.

In ideal situations every mentioned work area is available to the client by LTE-M multicast transmissions. As soon as the client-server communication is finished, the a multicast transmission to the other machines is started via LTE-M single cell point-to-multipoint operation. Every polygon in the new multipolygon is shared via the multicast service to every machine with the same GIs and PI in the MVSC system. As these machines operate together in a group on the same field and therefore need to know the areas, which were applied by other machines of the group, the polygon exchange via multicasting can reduce the server load.

The server is a full backup of any applied area, which can be used when a machine starts work at a later date or time. The server can transfer not only the PI, MI and GIs but also all the available polygons. Since the machine could have missed shared data from past multicast transmissions, the server can provide this knowledge in an initial update.

In some cases the general data traffic of the network can be reduced. Two drivers spraying on an rectangular field are operating in the same MVSC system with the same PI. In case they decide in a consultation before starting spraying, that they want to divide the field in half, only the polygons near the boundary between their working areas need to be exchanged. These polygons can easily be shared via the centralized server, as the server responds to the update request of the client by sending need, which area is fully or partly included in the computed circle.

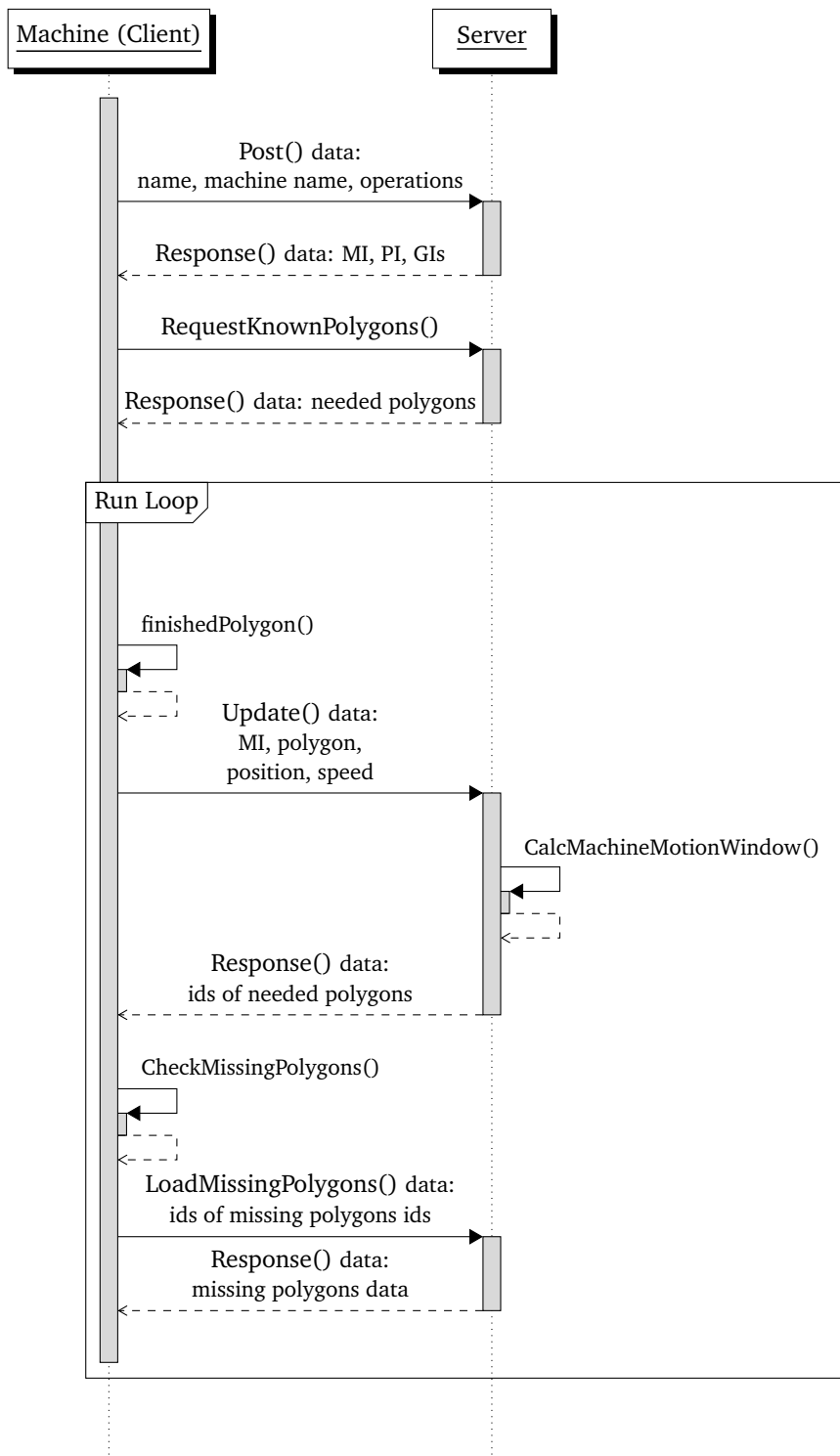


Figure 4.5 – Sequence diagram representing the communication of a machine with a centralized server

Nóbrega et al. [2] mention different protocols for the network layer, the transport layer and the application layer for Internet of Things developments in the context of smart farming. Among them is the Hypertext Transfer Protocol protocol, which is an application layer protocol. It operates on requests and responses. This architecture is suitable for this concept of a MVSC system, which can be based on a client-server network and thereby needs responses to the published data in requests.

4.4 LoRa - based P2P Network

Another possible solution for developing a MVSC system is based on the underlying LPWAN technology LoRa.

For sharing data among all machines a LoRa P2P network is established. Due to the possibility to send data over long distances and the cheap prices for devices LoRa can be regarded as a very suitable technology. It enables all vehicles to communicate with each other over the whole field. For this purpose, all tractors will be equipped with LoRa devices, which can have one or more channels. If the machines have this equipment, there are no further running costs as LoRa operates on the unlicensed spectrum. As no extra infrastructure is needed for this networking, this P2P communication can be set up very flexibly.

Since all machines will be equipped with LoRa devices, they can work together on any given field by broadcasting generated polygons, which represent applied areas. The ASC system of every machine can operate using the workareas received in a broadcast. This enables them to do joint cultivation.

But LoRa is only a physical layer implementation and therefore has no MAC layer implementation, which is needed in order to control the wireless network access. In this process, communication channels must be created for the individual machines. To prevent possible interference, individual LoRa units should not use the channels at the same time. Thereby it must be ensured that all devices have as much a sending time as possible. It is also desirable that the LoRa - based P2P network enables machines to re-send already shared polygons. This is necessary to inform machines, who missed polygon transmission, at a later date or to update new arriving machines about the cultivated areas.

LoRa offers different techniques to create non-interfering communication channels. By using additionally CDMA logical channels can be set up by using different SF for each channel. But every greater SF than 7 effects the data rate Equation (3.1) and therefore also the time on air. Lower data rates are not desirable, since the devices would then only be able to send less packets due to duty cycle limitations.

Frequencies in the range from 863 MHz ... 870 MHz are limited to a maximum duty cycle of 1 % by the german frequency plan [20] and therefore not suitable for this

use case. As an exception a 10 % duty cycle is offered for the usage of frequencies 869.4 MHz...869.65 MHz.

As many of the polygons are generated in around 3 s by the ASC system and sharing a polygons can take up to 1 s, a duty cycle of 1 % would not fulfill the requirements of being able to share every covered work area. Using a duty cycle of 1 % would also lead to a long break after every sharing process. This is undesirable because it can lead to long delays in the exchange of polygons.

As only the frequency band from 869.4 MHz...869.65 MHz with the 10 % duty cycle is suitable for this communication, it is impossible to use FDMA for implementing different transmission channels. An alternative is using TDMA, where every device gets a fixed time slot for sending data in the network.

The time slot is determined via the MI, as it is defined in Algorithm 4.1. The presented modulo 10 calculation results from the maximum number of 10 machines, which I have named as a system requirement. This means that each device is granted every a transmission time of 1 s every 10 s. So devices have to wait for their time slot in order to transmit on the logical channel provided by TDMA and thereby also wait to abide the duty cycle limitations of the german frequency plan[20]. But TDMA requires synchronizing the time of all operating machines. Otherwise time slots for broadcasting may overlap. This can be less problematic for a MVSC system of two operating machines, where a gap of 4 s can be kept between the sending time slots of the LoRa nodes. But an increasing number of machines in a MVSC system increases the probability of overlapping time slots.

A solution may be the usage of the Sensor MAC protocol which was designed by Ye, Heidemann, and Estrin [31]. Another possible solution for this problem is the self-organizing TDMA protocol which is defined by Derakhshani et al. [32]. Both protocols allow every node to observe the network situation and operate in it in a smart coexistence.

As every machine is equipped with a GPS receiver, GPS can also be used for time synchronisation. Lombardi [33] mentions that a time synchronisation within a few

Require: current seconds (0-59)

Ensure: synchronized time

```

1: machine id as  $M_{ID}$ 
2: current seconds as  $sec$ 
3: if  $sec \bmod 10 == M_{ID}$  then
4:   p2pCommunicationSend()
5: else
6:   p2pCommunicationReceive()
7: end if
```

Algorithm 4.1 – Determining time slot for sending

ns are possible. This makes the GPS time another suitable solution to the mentioned problem. But there may be interference while using TDMA. When two MVSC systems operate on neighbouring fields with the same LoRa parameters, there is a possibility that 2 machines try to send messages at the same time. As a result, a machine may only receive messages from the neighboring field because it is currently working along the field boundary and is therefore closer to machines of the neighboring field. In order to be able to separate the LoRa communication of the MVSC systems, different parameters can be set. If one systems uses SF6 and the other one SF7, the LoRa channels of each system can use TDMA and are isolated by CDMA. SF6 also enables an efficient data rate. Even SF8 can be listed in this context. However, significantly fewer duplicates can be sent with SF8.

Another possibility is using another frequency and thereby separating the channels by FDMA. LoRa can use the frequencies ranging from 433.050 MHz... 434.790 MHz. The german frequency plan [20] states no duty cycle limitations for these frequencies. But devices are limited to a TX power of 10 dBm (10 mW) while operating in this range. The devices would also have to be equipped with 433 MHz - suitable antennas. Nevertheless, it is a realistic and good differentiation option.

To achieve a high data rate for every LoRa transmission, a SF of 6 or 7, a CR of $\frac{4}{5}$ and a BW of 250 kHz is chosen for the LoRa P2P network. A higher SF is not suitable, because it would significantly reduce the data rate. A wider BW would be convenient for a better data rate. But the BW is limited to the 250 kHz frequency range from 869.4 MHz till 869.65 MHz, because it offers the highest possible duty cycle.

The set TX power effects the received signal strength and the resilience against possible path losses [22]. As the machines comply to the duty cycle limitation the maximum TX power for this frequency is 27 dBm (500 mW).

Every polygon is exchanged in the application data structure Section 4.2, which has been modified to fit into the LoRa frame structure. The amendments are visible in Figure 4.6.

After the preamble and the header the application data structure is integrated in the LoRa frame payload with a maximum size of 255 Byte. As LoRa already has a network identifier implemented in the *sync word*, the 4 Byte for the PI can be left out of the header of the application data structure. Every machine operating on the same field can use the same *sync word* instead of the PI. Any external message from outside of the LoRa-based P2P network on the same field contains a different *sync word* and can therefore be discarded as it is not relevant.

The LoRa frame has a limited payload size of 255 Byte which leads to other amendments to the application data structure. Some polygons can contain many coordinates, which would exceed the packet size. These polygons must be sent as a number of consecutive packets. Therefore the last 2 Byte added to the header of the

application data structure encodes an integer. It represents, which packet it is and the total number of packets to expect, by adding the total packet count multiplied by 10 and the packet number. 31 for example stands for the first of three needed packets for having all the coordinates of the polygon.

The simulation, mentioned in Section 3.4, generated polygons with 74 coordinates at the most, which would result in 592 Byte being encoded. This exceeds the maximum space for encoding coordinates of 248 Byte and therefore is sent in 3 consecutive packets. Their polygon identifier and sequence is encoded in the integers in the header. A LoRa receiver waits for all 3 packets and then just rebuilds the complete polygon.

To enable using the application data structure a MI and GIs have to be provided. These can be inserted by the driver and thereby provided to the software of the MVSC system in a machine.

Algorithm 4.2 explains the general behaviour of each machine and their LoRa device in the P2P network.

While a Lora node is not sending, it is in receiving mode. It continuously listens for packets of other vehicles. As soon as a message arrives, it is getting decoded and the *sync words* and GIs are being checked. In case of matching *sync words* and if any GIs are equal to the own GIs of the machine, the whole shared polygon is stored and used in the ASC system. This means that the polygon was broadcasted by a machine operating on the same field and doing the same operation. When a new workarea is generated by the ASC system and is ready for being shared, it is encoded in the defined scheme presented in Figure 4.6 and pushed into a message queue together with its calculated transmission time in ms. As soon as the time slot of the device is reached, the machines tries to transmit the messages waiting in the queue via LoRa. Before a message is sent, the machines checks if enough time is left to share the message. Therefore it checks whether the sending time is bigger than the precalculated message transmission time. Taking into account the aforementioned parameters and proposed data scheme the message transmission time can be calculated by using Equation (3.1) and add to it the time for sending the preamble and the mandatory preamble, which contains the *sync words*. The preamble is set to the default length of 8 symbols. This leads, according to Equation (3.2),

| 1 | 2 | 2 | 0-248 | 2 |
|-----------------------------|------------|------------|--------------------------------|-------------|
| <i>Preamble &Header</i> | New/GIs/MI | Polygon id | <i>n of m expected packets</i> | Coordinates |

Figure 4.6 – Amendments of the application data structure for the LoRa P2P network

to a transmission time of around 5.3 ms for both preambles. Therefore the total message transmission time is less than 190 ms for a sample polygon which contains 30 coordinates.

On the basis of this value and the polygon production time distribution Figure 3.5 as well as the distribution of number of coordinates in a polygon Figure 3.4 it is apparent that a machine has a lot of its sending time left, because most of it is not needed to share its polygons generated by the ASC system. This time is used for sharing old polygons known to the machine. They can either have been generated by the machine at an earlier time or been received from previous LoRa communications. Transmitting known polygons is very important to create redundancies. If a machine isn't able to reach all machines, because of a limited LoS due to obstacles or hilly terrain, some machine will need at least a second transmission to receive the polygon. This is highly needed as this concept contains no centralized server with a backup. Another use case of sending duplicates is to update new machines, joining the MVSC system about the treated workareas.

There are different strategies for selecting old polygons that are transmitted. They can of course be picked randomly.

However, more decision-making possibilities arise when the position of the other machines is taken into account. While a machine is receiving a shared new polygon,

Require: determined *timeSlot* for sending

- 1: Queue of newly produced polygons as *queue*
- 2: LoRa device in receiving mode
- 3: **if** *timeSlot* **then**
- 4: Sending Time as *sendTimeInMs* = 1000 ms
- 5: **while** *sendTimeInMs* > 0 **do**
- 6: **if** *queue* not empty **then**
- 7: Required sending time of new polygon as *reqTimeInMs*
- 8: *sendTimeInMs* = *sendTimeInMs* - *reqTimeInMs*
- 9: **if** *sendTimeInMs* > 0 **then**
- 10: Share polygon via LoRa
- 11: **end if**
- 12: **else**
- 13: Required sending time of old polygon as *reqTimeInMs*
- 14: *sendTimeInMs* = *sendTimeInMs* - *reqTimeInMs*
- 15: **if** *sendTimeInMs* > 0 **then**
- 16: Share old polygon via LoRa
- 17: **end if**
- 18: **end if**
- 19: **end while**
- 20: **end if**
- 21: LoRa device in receiving mode until next *timeSlot*

Algorithm 4.2 – Sharing data via LoRa in a machine's sending time slot

which is indicated in the second part of the header of the proposed data scheme, it can track its origin. As each arriving message contains a MI, the sender can be identified. The position of the sending node can be estimated by calculating the center of the last transmitted new polygon. This allows each machine to roughly assess the position of other machines. This way a machine is able to detect when two machines are very far apart. To help out possible failed transmissions between them, it can repeat the polygons, the MI and GIs of the mentioned two machines. Another possible strategy is useful for updating a new machine, joining the MVSC system. As soon as the new machine arrives at a field, it can share its MI, GIs and just its position, instead of coordinates of a polygon. As a result, all other machines recognise the new working unit and can share old polygons, which represent the areas near the transmitted position. This is necessary for the new unit, as it should not treat the transmitted workareas a second time. As each machine listens to every transmitted message, each is aware of the current knowledge of the new machine and can send another required polygon.

After presenting the two concepts for MVSC systems, I conduct a simulation for each concept and a LoRa field experiment in the agricultural domain to evaluate the two solutions.

Chapter 5

Evaluation

5.1 LoRa test environment

The success of a LoRa communication and therefore also the feasibility of the proposed LoRa-based MVSC system depends on the settings chosen and the environment. In order to test LoRa communication in an agricultural domain I conducted the following measurements.

Every field can have so-called islands. These can be woods, farm buildings, antenna towers or transmission towers in the field. They are obstacles in the Fresnel Zone, which can lead to signal energy loss. The effects vary by their heights, diameters and density. Agricultural machines work in various terrains, where valleys and hills can cause loss of sight during communication. In order to test the mentioned ambient effects on the LoRa P2P network, different experiments are carried out. The tests are conducted in flat and hilly regions around different obstacles to the LoS-communication.

For the experiments *LILYGO TTGO T-Beam V1.1 ESP32 LoRa* - capable devices operating on frequencies around 868 MHz are being used. The product is distributed together with 3-dimensional uniform array antenna, which will be used as well. A 3-dimensional uniform array antenna is explained in [34]. Such an antenna uses a 3-dimensional structure as a radiation pattern or antenna pattern. It can be achieved by stacking multiple planar arrays on the z axis.

Mounting an antenna as high up as possible can improve long range communications, because it makes keeping the Fresnel Zone free of obstructions much easier. On basis of the regulation in StVZO §32 Abs. 2 every agricultural vehicle or combination of vehicles must be less than of 4 m tall. This already limits the antenna height. But as agricultural tractors and machinery working on a field of up to 300 ha can be considered to have a height of 3 m and every communication antenna can easily be placed on the highest point of a machine, the LoRa Communication is tested at this

height.

For the experiments the LoRa nodes are mounted on top of a 3 m wooden pole with the antenna as an extension directed upwards, as it is visible in Figure 5.1. The devices are attached to a Notebook via a 3 m long micro USB to USB 2.0 cable. This supplies them with power and also provides serial communication, which is used to transfer any sent or received data to the notebook, where it is logged.

As agricultural vehicles usually operate on a field moving not faster than 20 km/h (5.6 m/s), the Doppler Effect on the LoRa communication can be regarded as negligible and therefore a static experiment setup can be used.

For programming the LoRa devices for the conducted tests I used the library *arduino-LoRa*³. It is open source on MIT licence. I carried out the experiments using the SF7,

³An Arduino library from Sandeep Mistry <sandeep.mistry@gmail.com> for sending and receiving data using LoRa radios. <https://github.com/sandeepmistry/arduino-LoRa.git> Version: 0.8.0



Figure 5.1 – Experimental setup LoRa sender

the CR 4/5 and a BW of 250 kHz ranging from 869.4 MHz...869.65 MHz, because the suggested LoRa P2P network will operate on these parameters. As declared in the german frequency plan [20] it is allowed to operate devices with TX power of 500 mW accessing this frequency range. The used devices are configured to send with 20 dBm 100 mW, as these devices are limited to this sending power.

I configured the sending device to send a 248 Byte package every second. This correlates to 30 coordinates in polygon, which are encoded in a 8 Byte header and a payload of 240 Byte. For this series of experiments a different previous version of the data structure was used. Therefore the header is 8 Byte instead of the defined 9 Byte of the data scheme.

For the conducted experiments the header contains an integer counting from 1 to 100. After the integer reaches 100 it starts again at 1. At every measurement position the receiving node tracks every received packet and their Received Signal Strength Indicator (RSSI). After the experiments a random selection of packets with the integer ranging 1 to 100 is chosen. From this, a PRR is derived.

For calculating the average RSSI I used all the measured values of all received packets.

The Devices are positioned in various distances from each other in different settings, to test the behaviour of the LoRa communication in these places.

In order to track the position of every measurement unit, I used a smartphone gps sensor together with the app *GPSData* in version 2.1.01.240. The application is developed by examobile and offers an accuracy value for this smartphone of less than 5 m, which is achieved for the getting the position of the devices. From this GPS data, the distance and the height difference between the LoRa nodes can then be calculated.

For the first series of measurements I chose a flat area near Burgstall (52°24'13.968"N, 11°41'5.136"E) in Germany. In experiment 1 I placed the devices a tower of a powerline, which is shown in Figure 5.2.

During the experiments 2, 3 and 4 I placed the sending device in front of snow-covered pine tree forest, while the receiving node is moved gradually deeper into the woods. This setup, visible in Figure 5.3, again aimed to test the behaviour of LoRa communication, while having an obstruction in the LoS.

I conducted the next series of tests with the numbers 5 to 7 on the open ground. As displayed in Figure 5.4 sender and receiver are located with different distances from each other. Thereby a maximum distance of 2060 m was reached in experiment 7. Studying the LoRa communication over so long ranges it was impossible to keep the Fresnel zone completely obstacle-free. Bushes and large trees grew near the streams, marked blue in Figure 5.4, and tree avenues surrounded roads, visible in white and yellow in Figure 5.4.

During the mentioned measurements the sky was partly cloudy, the terrain was

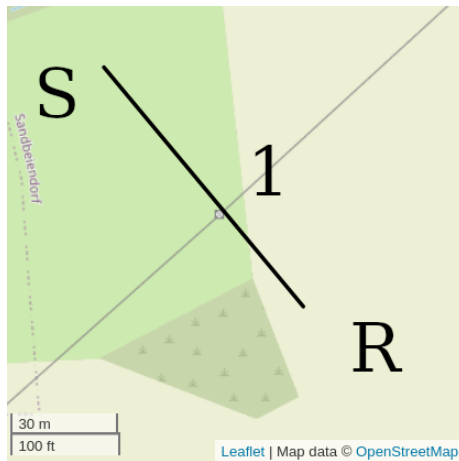


Figure 5.2 – Experiment setup 1 for measuring around power tower, symbolized by the black line between sender and receiver. Base map and data from OpenStreetMap and OpenStreetMap Foundation

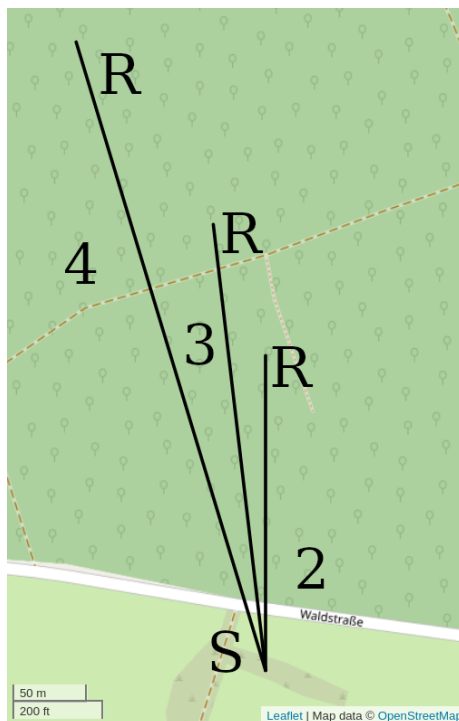


Figure 5.3 – Experiment setups 2 to 4 for measuring in a forest. Base map and data from OpenStreetMap and OpenStreetMap Foundation



Figure 5.4 – Experiment setups 5 to 7 for measuring in the flat countryside.
Base map and data from OpenStreetMap and OpenStreetMap Foundation



Figure 5.5 – Receiving LoRa device mounted on a tractor

covered with 0.2 m of snow and the temperature was below 0 °C (273.15 K). I chose an area near Weckersdorf ($50^{\circ}36'55.1016''N$, $11^{\circ}54'36.1116''E$) in Germany for experimenting in a hilly region. The sending node is placed in the middle of a field below a small hill. Whereas I mounted the receiving devices on a wooden pool on a tractor at a height of 3 m which is shown in Figure 5.5. Through it the receiver is mobile and able to drive to the different locations shown in Figure 5.7 and Figure 5.6. Thereby I moved the receiving node up and over a long hill, passing different bushes and small forests. A maximum distance of 2325 m between sender

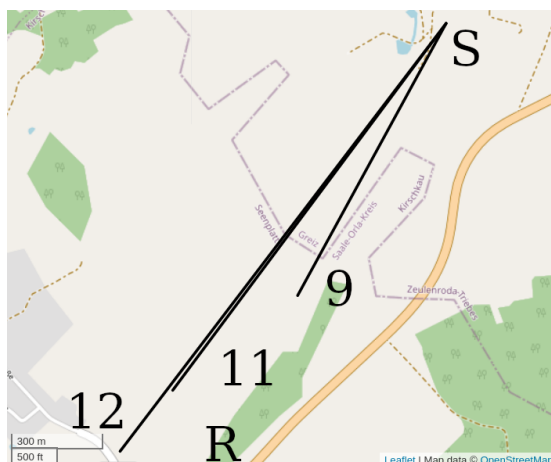


Figure 5.6 – Experiment setups 9, 11 and 12 for measuring on a hilly field.
Base map and data from OpenStreetMap and OpenStreetMap Foundation

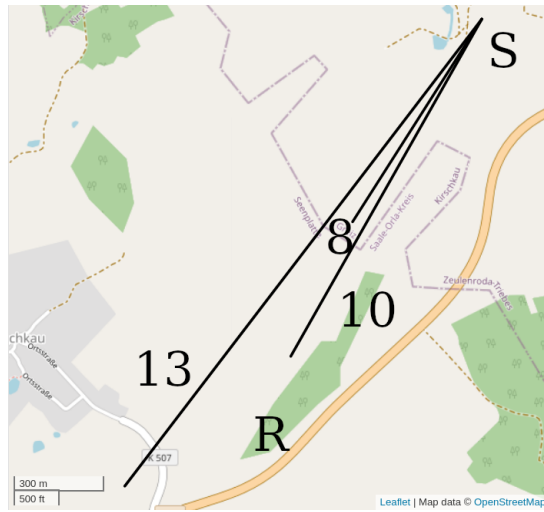


Figure 5.7 – Experiment setups 8, 10 and 13 for measuring on a hilly field.
Base map and data from OpenStreetMap and OpenStreetMap Foundation

and receiver with an altitude difference of 90 m was reached in experiment 13 which is shown in Figure 5.7.

In addition to the experiments on the transmission effects from an agricultural working environment I also tested the interference of several transmitters. In practice, it may happen that MVSC systems are used on two adjacent fields at the same time. It

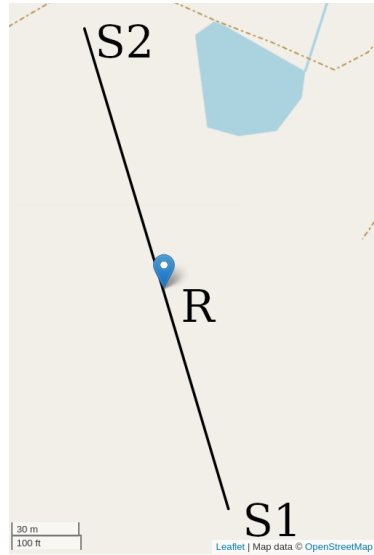


Figure 5.8 – Experiment setup for testing interference of two senders using the same transmission parameters, where the marker represents the position, where the received signal switched from S1 to S2. Base map and data from OpenStreetMap and OpenStreetMap Foundation

could happen that at least two machines are transmitting concurrently. In order to test this setting and its consequences another experiment is conducted.

Two senders are configured to simultaneously send a 16 Byte message every 100 ms. The message contains two different integers, which serve as sending device identification. SF, BW, CR and TX power are set to the aforementioned values. The two sending nodes are placed on a open ground at a distance of 230 m. The receiver mounted on the tractor is driven with less than 10 km/h (2.78 m/s) from sender 1 to sender 2. The whole test setup is shown in Figure 5.8.

During this it was observed that up to the marker on the map, only the signal from transmitter 1 was received. After that, the signal changed so that only packets from sender 2 were received. The marker had a distance of 120 m to sender 1 and a distance of 100 m to sender 2.

5.2 LoRa test results

The following section presents the results of the LoRa experiments. All plots are without any confidence intervals, because the average RSSI values have small confidence interval, which are not wider than 0.5 dBm. The results of experiment 1 are visible in Table 5.1. 100 % of the packets were received. It can be concluded that a powerline tower is not a potential concern for LoRa communication.

A PRR of around 100 % was also achieved during the conducted experiments 2 to 4 in the pine tree forest. Their outcome is recorded in Table 5.2. The RSSI value decreased linearly during the test in the forests which is shown at Figure 5.9. Nevertheless this reveals that despite the additional layer of snow on the trees, reliable LoRa communication is possible over short distances of up to 400 m. However, the RSSI value of experiment 4 at 440 m in the forest was almost as low as in the open flat field at a distance of 2060 m during experiment 7. This clearly implies that the

| Experiment | Distance | PRR | RSSI |
|------------|----------|-------|---------|
| 1 | 80 m | 100 % | -64 dBm |

Table 5.1 – Results of experiment 1, where LoRa was tested around a powerline towerFigure 5.2

| Experiment | Distance | PRR | RSSI |
|------------|----------|-------|----------|
| 2 | 210 m | 99 % | -84 dBm |
| 3 | 300 m | 100 % | -95 dBm |
| 4 | 440 m | 100 % | -109 dBm |

Table 5.2 – Results of experiments 2 to 4, where LoRa was tested in varying distances in a pine tree forest Figure 5.3

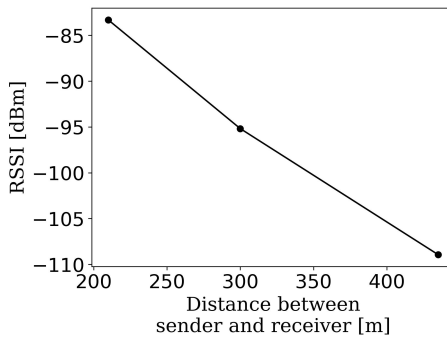


Figure 5.9 – Results of experiments 2 to 4, where LoRa was tested in varying distances in a pine tree forest Figure 5.3, represented as the RSSI regarding to the distance between sender and receiver

LoRa signal suffers a high path loss in the forest.

Despite the Non-Line-of-Sight communication due to occasional trees and houses during the experiments 5 to 7 in the open flat area around Burgstall ($52^{\circ}24'13.968''N$, $11^{\circ}41'5.136''E$) a PRR of around 100 % was measured. Their outcome is presented in Table 5.3.

It is visible in Figure 5.10 that the RSSI value drops faster from the second measurement on. The altitude data shows that during the third measurement LoRa messages were sent over a small hill, which could be a reason for the faster drop. The conducted experiments 8 to 13 in the hilly countryside resulted in a measured average PRR of around 99 %. The longest distance thereby was 2325 m on an difference of altitude of 90 m. During this series of measurements, no further packets could be received at a greater distance. This may be due to the fact that there would then have been a large long hill between the transmitter and the receiver.

The complete results of these tests are presented in subplot (a) of Figure 5.11. As

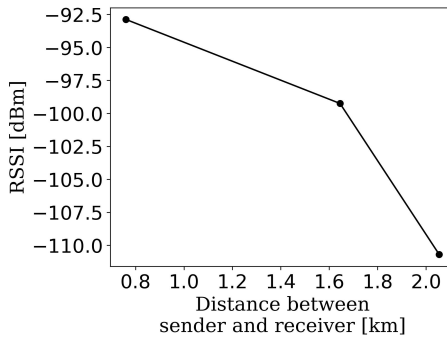


Figure 5.10 – Results of experiments 5 to 7, where LoRa was tested in different distances in the flat countryside of northern Germany Figure 5.4, visualized as the RSSI regarding to the distance between sender and receiver

| Experiment | Distance | Δ Altitude | PRR | RSSI |
|------------|----------|-------------------|-------|----------|
| 5 | 760 m | 0 m | 100 % | -92 dBm |
| 6 | 1645 m | 13 m | 100 % | -99 dBm |
| 7 | 2060 m | 12 m | 99 % | -110 dBm |

Table 5.3 – Results of experiments 5 to 7, where LoRa was tested in different distances in the flat countryside of northern Germany Figure 5.4

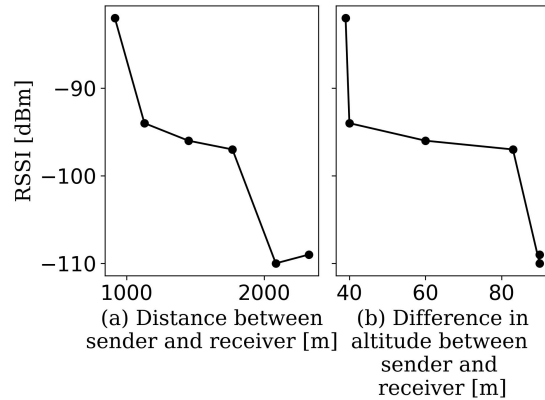


Figure 5.11 – Results of experiments 8 to 13, where LoRa was tested in different distances in the hilly countryside of Mid-Germany, represented as the RSSI regarding to (a), the distance between sender and receiver and (b) their difference in altitude

| Experiment | Distance | Δ Altitude | PRR | RSSI |
|------------|----------|-------------------|-------|----------|
| 8 | 915 m | 39 m | 100 % | -82 dBm |
| 9 | 1130 m | 40 m | 99 % | -95 dBm |
| 10 | 1450 m | 60 m | 99 % | -97 dBm |
| 11 | 1770 m | 83 m | 100 % | -97 dBm |
| 12 | 2085 m | 90 m | 100 % | -110 dBm |
| 13 | 2325 m | 90 m | 99 % | -109 dBm |

Table 5.4 – Results of experiments 8 to 13, where LoRa was tested in different distances in the hilly countryside of Mid-Germany Figure 5.7/ Figure 5.6

can be observed in subplot (b) of Figure 5.11, the RSSI value has hardly changed between the measurements 9 to 11. During the experiments 8 to 13 the LoRa receiver mounted on a tractor was driven up a long and flat hill. In the measurements 9 to 11, the tractor was ascending the hill, so fewer obstacles were in the LoS between sender and receiver, which did not increase the path loss too much. In contrast, measurements 11 and 12 were conducted on the top of the hill and therefore contained parts of the hill in the Fresnel zone, which led to a significant decline in the RSSI value.

The last experiment on interference revealed that a receiver almost always hears the sender who is closest. In the results, the receiver is not quite in the middle between the two transmitters at the point of switching. This may be due to measurement uncertainties caused by movement with the tractor or the slightly uneven terrain.

5.3 Simulation studies

After testing LoRa in the agricultural domain I conducted simulation studies to proof the concept and investigate the effects of the system's design decisions.

Simulation of the broadcast-based concept

The first study simulates the LoRa-based MVSC system. The suggested solution consists of a LoRa P2P network, where polygons are shared via broadcasts. To prevent interference every LoRa node gets assigned a time slot for sending. To achieve a higher system reliability duplicated messages need to be shared among the peers, in case of a lost communication. Duplicates are also needed to update new members of the P2P network.

In order to simulate the LoRa network and its possibilities, *OMNeT++*⁴ is used. Every LoRa Device is represented as a node, which is connected to every other node. Every node can send for 1 s every 10 s. An example network of 5 nodes is shown in Figure 5.12.

The simulated polygons are based on the data from the field, shown in Figure 3.3. It is the 210 ha area near Fraßdorf ($51^{\circ}43'40.4004''N$, $12^{\circ}6'43.272''E$) in Germany. During the simulation every node generates polygons in varying time intervals, based on the distribution which is represented in Figure 3.5. Therefore every node chooses a random integer between 0 and 581, which is used as an index for an array containing all simulated polygons with their number of coordinates and their production time. Then the node waits for the production time until it starts again choosing a new random number as an index.

This allows the LoRa communication to be simulated on data retrieved from a real

⁴<https://omnetpp.org/> version: 5.6.2

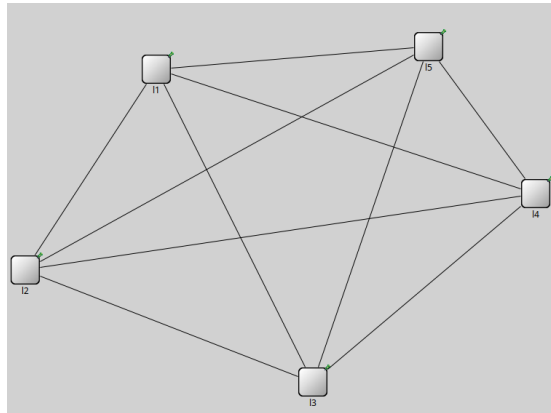


Figure 5.12 – OMNeT++ simulation network of 5 nodes

field.

Every node stores the generated polygons in a queue and uses the Algorithm 4.1 to determine its time slot for sending. When it is its turn to send, it operates as it is described in Section 4.4 and visualized in the Algorithm 4.2 to share data. First the node tries to send every polygon in the queue. If there is still some time for the node left for sending, it starts sending old and known polygons. They are simulated the same way. The node chooses a random integer as an index for the array containing all the simulated polygons.

Every channel between the nodes is of the type *cDelayChannel*. This channel type allows a variable transmission time to be set for each channel. If a node wants to send a polygon, it uses the number of coordinates in the polygon to calculate its required consecutive packets and sums up their transmission time. Then it sets the channel delay to the sum. This allows the time on air per polygon to be simulated. The simulation runs for at least 120 min. Every 2 min it tracks the new polygons sent, the old and known polygons sent, the new polygons received and the old and known polygons received.

To simulate packet loss, individual channels could be disabled randomly for the period of a transmission. Since the test results lead to the conclusion that there will be almost no packet loss on a normal field, this is omitted.

Simulation results of the broadcast-based concept

The LoRa P2P network was simulated in order to track the possible network data sharing capacity. As shown in Figure 5.13 around 85 polygons in varying sizes were distributed by every simulated node in 60 min. This number is limited to the generation of new polygons. If the ASC system produces more, more polygons can be transmitted.

The potential capacity for sharing additional polygons in terms of time is visible in Figure 5.14. An average of 1430 polygons were sent by every simulated node in 60 min. The total number of sent polygons in 60 min per node is on average around 1515. This is more than 2.5 times the number of all polygons of the simulated 210 ha area near Fraßdorf ($51^{\circ}43'40.4004^{\prime\prime}$ N, $12^{\circ}6'43.272^{\prime\prime}$ E) in Germany, shown in Figure 3.3.

There are no significant differences in the number of polygons sent per node in relation to the network size. This was to be expected, as each node attempted to make the best possible use out of its transmission time.

In contrast, there is a big difference in the number of messages received depending on the number of nodes in the network. As visible in Figure 5.15 and in Figure 5.16

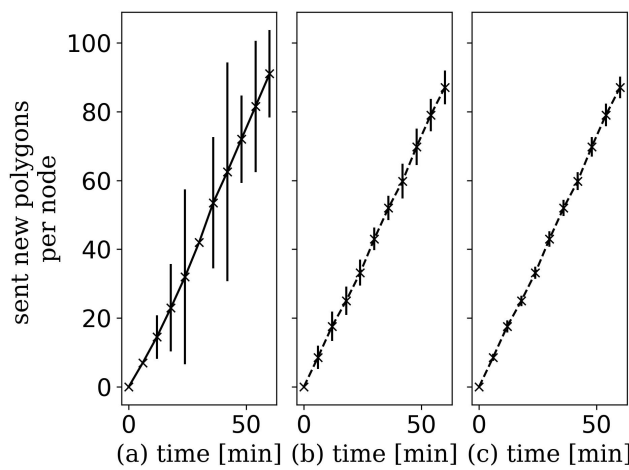


Figure 5.13 – LoRa P2P network simulation results, showing the number of sent new polygons per LoRa node with regards to the time, (a), (b) and (c) contain 2, 5 and 10 respectively.

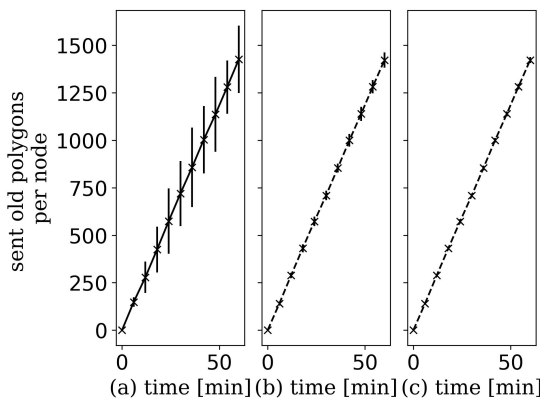


Figure 5.14 – Ditto for old / known polygons

a LoRa node in a network with 10 communication participants received a lot more than a node in a 2-node-network. This was to be expected, since a node in a larger network receives data from many more other nodes.

As the sending of duplicates is used to update new machines, it has to be evaluated, how quickly a network has transferred the required data. A new machine can join a MVSC system controlling 5 machines and would be able to receive around 190 polygons in 2 min. This amount equals to one third of the total polygons of the mentioned field near Fraßdorf ($51^{\circ}43'40.4004''\text{N}$, $12^{\circ}6'43.272''\text{E}$) in Germany.

To be sure that each machine has received all the polygons sent, it is necessary to send duplicates again. This way, if the first possible transmission of the polygon did not work, there is a second chance to share this polygon. If the simulation results

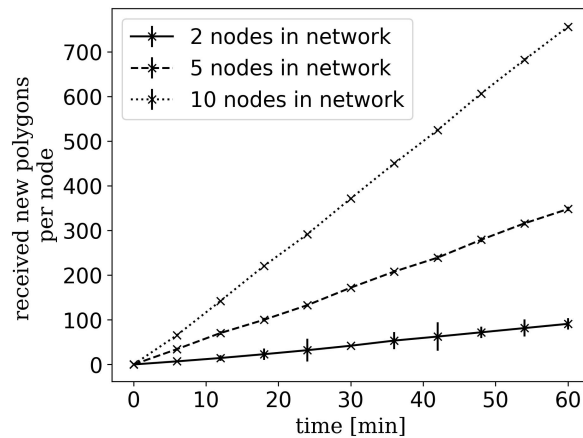


Figure 5.15 – LoRa P2P network simulation results, showing the number of received new generated polygons per LoRa node with regards to the time

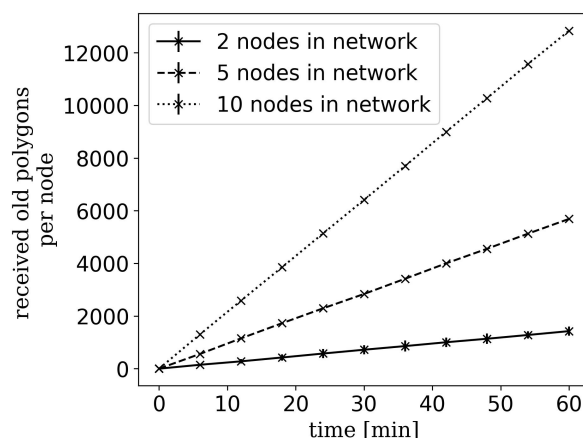


Figure 5.16 – Ditto for old / known polygons

are considered, it can be seen that a participant of the network with 2 nodes has received 90 new polygons and over 1400 old polygons in a time of 1 h. This means that the network has the capacity to repeat each new polygon over 15 times. In a network with more nodes, the ratio increases even more.

Simulation of the client-server-based concept

After testing and simulating the characteristics of the LoRa-based MVSC system, I analysed the design decisions of the LTE-M-based concept.

A significant difference comparing the two concepts is the centralized server in the LTE-M-based MVSC system. In order to simulate the impact of such a centralized server, I simulate a prototype of the LTE-M-based MVSC system. It features only the client-server-logic. Therefore the multicast option is not implemented. It contains two clients and a server, which are hosted in a local network and have user interfaces, which visualize the applied areas as polygons on *OpenStreetMapss*.

The two clients represent two machines which were configured to operate together in group 3. At the beginning, as suggested in the proposed MVSC system each client sent an post request with the data which contains the name, machine name and groups, to the server. The data was set in the user interface of each client. The server responds to each client with their MI and GIs. As only one field with two clients and a server is simulated, no PI is needed and the PI is omitted.

For the conducted simulation polygons from the simulated field near Fraßdorf ($51^{\circ}43'40.4004''\text{N}$, $12^{\circ}6'43.272''\text{E}$) are used. As a tractor was simulated driving along a GPS trace over the field near Fraßdorf the simulated polygons were generated sequentially following the path. For this simulation of the LTE-M-based MVSC system these sequential polygons are inserted in the client applications every 2 s. As I only analysed the impact of the polygon exchange via the server, I chose a polygon production interval of 2 s to speed up the simulation.

The complete amount of polygons used for the simulation is shown in Figure 5.17. The first client was simulated to start in the left of this area. The whole working area of the first client is indicated in black in Figure 5.18. It ought to work until the second client starts, which is represented in blue in Figure 5.18. The whole working area of the second client is shown in black in Figure 5.19.

This setup represents two machines, which share one common border of their workareas. As the second client is first operating along this border, it defines the exact location of the border. During its operation it moves away from this border, therefore doesn't need to know any of the polygons of the first client, because it is not likely to treat an area of the first client. While the first client is advancing towards this border, it has to know the polygons of the second client.



Figure 5.17 – Applied polygons of group 3 (Machine 1 and Machine 2), which are tracked by the server. Base map and data from OpenStreetMap and OpenStreetMap Foundation



Figure 5.18 – OpenStreetMap representing known polygons of Machine 1, where the black polygons are the applied areas of Machine 1 and the blue polygons show the applied polygons of other participants of group 3 (Machine 2). Base map and data from OpenStreetMap and OpenStreetMap Foundation



Figure 5.19 – Ditto for Machine 2. Base map and data from OpenStreetMap and OpenStreetMap Foundation

Therefore the two clients and the server operate on basis of the logic described in Figure 4.5. The two clients send their polygons to the server, which tracks and presents the applied polygon in blue in the *OpenStreetMaps* shown in Figure 5.17. The server responds to every client update with a list of polygon identifiers and their corresponding MI, that the client will need to know while advancing. Otherwise the client could operate on the area a second time.

As no exact positon, motion direction and speed is simulated, the radius of the motion window, shown in Figure 4.4, is set to a fixed constant of 150 m. The centre of the motion window is set to the calculated centre of the transmitted polygon of the clients update.

When a client needs to load missing polygons which were specified by the server, it requests them from the server and represents them in blue in its *OpenStreetMaps*. This set of shared polygons is much smaller than all polygons used in the simulation Figure 5.17.

Simulation results of the client-server-based concept

Via multicast or broadcast transmissions every applied area is shared and thereby supposed to be known to every machine. But this is not necessary for joint cultivation. Only if a machine is near an already treated area, it has to be aware of the corresponding polygons. That means, when a machine never operates in a section of a field, it has to have no knowledge about the operations being carried out there. A centralized server, knowing every applied area, can be used to just transmitted the needed polygons. This impact is indicated in the results of the previous simulation of the client - server connection. Only when the first client was moving near the already applied polygons of the second client, it had to know them. These polygons were successfully provided by the server. They are shown in blue, whereas the black polygons indicate the own generated polygons in Figure 5.18.

5.4 Comparison of the MVSC systems

After testing and simulating the LoRa P2P network in different scenarios and testing a prototype of the LTE-M based MVSC system both concepts are compared now. Thereby the network coverage, data rate, costs, backup options and potential issues of both proposed MVSC systems are compared with each other. Backup options specifies a part of the proposed system, that is able to recover all applied polygons. This may be needed, when a machine joins a field and needs to know the already applied areas at a later time. Potential issues mention problems that can to occur. During comparison the LoRa-based P2P network is referred to shortly as LoRa-based and the other concept is shortly named LTE-M-based.

Coverage

LoRa-based:

Conducted experiments in this paper indicate that LoRa is an applicable LPWAN technology for IVC in the agricultural domain. A PRR of at least 99 % was achieved while testing LoRa in a hilly countryside over a distance of 2.3 km with a difference in altitude of 90 m and no LoS between sender and receiver. It indicates that LoRa can enable agricultural machines for data exchange over long range. Even while testing LoRa over a distance of 440 m in a pine tree forest a PRR of 100 % is achieved. It shows that small woods in a field are very unlikely to disturb LoRa communication. As no additional infrastructure, except for LoRa devices, are needed to start the Lora P2P network, the LoRa - based MVSC system can be regarded as infrastructure independent and therefore can function in every region.

LTE-M-based:

A study conducted in Denmark pointed out, that LTE-M has a 99.9 % outdoor coverage [11]. However, to the best of my knowledge no LTE-M coverage measurements for Germany are available. The *Deutsche Telekom*, which is a german MNO, offers a coverage map on their website⁵. It shows some small areas in the countryside where there is no LTE-M coverage. But these rural areas are needed for the concept of LTE-M - based IVC in an agricultural domain. LTE-M relies on the infrastructure provided by the MNO. In case of this infrastructure not being available in some areas, because of for example base stations are out of operation, LTE-M can't be used in these areas.

Data rate

LoRa-based:

The LoRa device data rate for the mentioned parameters is around 10.9 kbit/s. Due to the duty cycle limitation of the frequency plan [20], a LoRa device is not allowed to send data at all time. The simulation concluded that this data rate with the duty cycle limitation is still enough for the MVSC system. The simulation shows that a machine is able to send up to 16 times the amount of its applied polygons. This suggests that the LoRa P2P network would be able to broadcast other data suitable for coordinating joint cultivation of multiple machines.

⁵<https://t-map.telekom.de/tmap2/mobileiot/>

LTE-M-based:

LTE-M offers instantaneous peaks of a data rate of up to 1 Mbit/s [12]. An also sufficient data rate of 180 kbit/s would still be available at a distance of 40 km between LTE-M device and base station according to the simulation described in [14].

Cost**LoRa-based:**

Depending on the hardware, different purchase prices of LoRa devices can occur. Ji and Yang [29] state, the LoRa industry can offer modules for prices between 7\$ and 10\$. But as the LoRa P2P network needs no additional infrastructure and operates in the unlicensed sub-gigahertz radio frequency bands no additional operating costs will arise. Additional costs may involve installing and setting up the LoRa Devices.

LTE-M-based:

The price for LTE-M devices also depends on the hardware. [12] states, that the prices to be expected are less than 10 \$. But additional costs arise for the usage of the needed infrastructure. Internet of Things tariffs for Germany are offered by the *Deutsche Telekom*, which is a german MNO. Over 3175 € have to be paid for 100 so-called *Business Smart Connect M2M L (eSIM)* LTE-M tariffs⁶, which enable sending a total amount of 3 GByte in a time of 36 months. Additional costs may arise for an internet connection of the server or the server hosting, as well as any support or services needed for setting up or updating the solution.

Backup options**LoRa-based:**

As the test results suggest a very promising PRR and the simulations indicated a high network capacity to exchange duplicates of each generated polygon, every machine can be regarded as a full backup of all applied areas

LTE-M-based:

When polygons are shared via LTE-M multicast transmissions, every polygon is also known all machines. However, if LTE-M only operates on client - server - communications, the server is the only full backup for all applied areas.

⁶<https://smart-connect-shop.iot.telekom.com/tdg-shop/shop/cart>

Potential issues

LoRa-based:

As the LoRa-based P2P network relies on TDMA to enable non-interfering communication channels, it requires synchronized time of all operating machines. But there are different possible protocols like the Sensor MAC protocol [31] or the self-organizing TDMA protocol [32] to enable TDMA for the proposed LoRa-based P2P network. In addition, the GPS receivers on each tractor can also be used for time synchronisation, because it makes time synchronization within ns possible [33].

LTE-M-based:

When the LTE-M - based Client - Server Network only operates on client-server-communications, the server is the only full backup for all applied areas. The concept of the LTE-M - based Client - Server Network heavily relies on the server. In case of the server being out of operation, the MVSC system won't be able to operate.

Chapter 6

Conclusion

In order to enable joint cultivation for multiple machines, I developed two concepts for Multi Vehicles Section Control (MVSC) systems. Both concepts enable the machines to exchange polygons to operate with Automatic Section Control (ASC) systems on basis of common knowledge of treated areas on the field.

The first proposed MVSC system consists of a client-server-network. Due to the underlying LTE-M connection, every machine can send its polygons to the server and additionally multicast its polygons to other machines on the field. A conducted simulation study in this work indicated that a centralized server can reduce the number of shared polygons. As the server tracks all polygons, it can provide only the polygons needed for every machine to operate on already treated areas. A multicast or broadcast also shares polygons, that are not essentially needed when the machine does not operate near the corresponding area.

The second concept for a MVSC system is a LoRa-based Peer-To-Peer Network (P2P network). Every machine is equipped with a LoRa-Device, which can broadcast applied polygons. As LoRa only implements a physical layer a sending time slot is assigned to every machine to operate under Time-division Multiple Access (TDMA). I performed a simulation study in order to evaluate the potential number of sent and received polygons per machine. The results indicated that every machine is capable to broadcast 16 times the number of polygons, it usually generates while operating on a field. This enables a machine to send duplicates of already shared polygons in order to update new joining machines or to add redundancy for failed broadcasts. With field measurements in a flat and hilly countryside I analysed the feasibility of LoRa in an agricultural environment. The maximum measured distance for LoRa communication was 2325 m with an altitude difference of 90 m. A field can contain small forests. This may result in two vehicles on a field having to communicate without a line of sight. Therefore I also measured the LoRa communication range in a pine tree forest, where I achieved a maximum range of 440 m.

The comparison of both solution pointed out, that the LoRa-based system is cheaper and more independent from any additional infrastructure than the LTE-M based concept.

Future work could investigate whether LoRa or LTE-M can be used for other use cases of Inter-Vehicular Communication (IVC) in the agricultural field.

List of Abbreviations

| | |
|--------------------|---|
| ASC | Automatic Section Control |
| BW | Bandwidth |
| CDMA | Code-Division Multiple Access |
| CE | Coverage Enhancement |
| CR | Coding Rate |
| CRC | Cyclic Redundancy Check |
| CSS | Chirp Spread Spectrum |
| ERP | Equivalent Radiated Power |
| FDMA | Frequency-Division Multiple Access |
| GIs | Group Identifiers |
| GPS | Global Positioning System |
| IVC | Inter-Vehicular Communication |
| LoS | Line-Of-Sight |
| LPWAN | Low Power Wide Area Networking |
| LTE | Long-Term Evolution |
| M2M | Machine-To-Machine |
| MAC | Media Access Control |
| MI | Machine Identifier |
| MNO | Mobile Network Operator |
| MVSC | Multi Vehicles Section Control |
| P2P network | Peer-To-Peer Network |
| PI | Process Identifier |
| PRR | Packet Reception Ratio |
| RSSI | Received Signal Strength Indicator |
| SF | Spreading Factor |
| TDMA | Time-division Multiple Access |
| TX power | Transmission Power |
| WAN | Wide Area Network |
| WAVE | Wireless Access in Vehicular Environments |
| WGS-84 | World Geodetic System from 1984 |

List of Figures

| | | |
|-----|--|----|
| 3.1 | Fresnel zone, which can be described as a cylindrical ellipse between sender and receiver devices | 10 |
| 3.2 | Screenshot LC:NAVGUIDE / A simulated tractor turns of boom sections, while passing an already treated area. | 12 |
| 3.3 | OpenStreetMap, which represents the multipolygon coverage of a single sprayer with a span of 36 m operating on a 210 ha - field. Base map and data from OpenStreetMap and OpenStreetMap Foundation | 13 |
| 3.4 | Distribution of number of coordinates per polygon on the simulated field | 13 |
| 3.5 | Distribution of the polygon creation time on the simulated field | 13 |
| 3.6 | Average number of coordinates in polygons in regards to the creation interval of the polygons on the simulated field | 14 |
| 4.1 | OpenStreetMap, showing a field shape with various indentations, where forests grow. Base map and data from OpenStreetMap and OpenStreetMap Foundation | 16 |
| 4.2 | Application data structure in Byte to encode and identify polygons in a MVSC system | 17 |
| 4.3 | 1 Byte where the first 4 bit are used as flags and indicating a new polygon and the participating groups and the last 4 bit encode the MI | 18 |
| 4.4 | Motion window until next position update depending on postion and a positive maximum speed | 20 |
| 4.5 | Sequence diagram representing the communication of a machine with a centralized server | 21 |
| 4.6 | <i>Amendments</i> of the application data structure for the LoRa P2P network | 25 |
| 5.1 | Experimental setup LoRa sender | 29 |
| 5.2 | Experiment setup 1 for measuring around power tower, symbolized by the black line between sender and receiver. Base map and data from OpenStreetMap and OpenStreetMap Foundation | 31 |

| | | |
|------|---|----|
| 5.3 | Experiment setups 2 to 4 for measuring in a forest. Base map and data from OpenStreetMap and OpenStreetMap Foundation | 31 |
| 5.4 | Experiment setups 5 to 7 for measuring in the flat countryside. Base map and data from OpenStreetMap and OpenStreetMap Foundation | 32 |
| 5.5 | Receiving LoRa device mounted on a tractor | 32 |
| 5.6 | Experiment setups 9, 11 and 12 for measuring on a hilly field. Base map and data from OpenStreetMap and OpenStreetMap Foundation | 32 |
| 5.7 | Experiment setups 8, 10 and 13 for measuring on a hilly field. Base map and data from OpenStreetMap and OpenStreetMap Foundation | 33 |
| 5.8 | Experiment setup for testing interference of two senders using the same transmission parameters, where the marker represents the position, where the received signal switched from S1 to S2. Base map and data from OpenStreetMap and OpenStreetMap Foundation | 33 |
| 5.9 | Results of experiments 2 to 4, where LoRa was tested in varying distances in a pine tree forest Figure 5.3, represented as the RSSI regarding to the distance between sender and receiver | 35 |
| 5.10 | Results of experiments 5 to 7, where LoRa was tested in different distances in the flat countryside of northern Germany Figure 5.4, visualized as the RSSI regarding to the distance between sender and receiver | 35 |
| 5.11 | Results of experiments 8 to 13, where LoRa was tested in different distances in the hilly countryside of Mid-Germany, represented as the RSSI regarding to (a), the distance between sender and receiver and (b) their difference in altitude | 36 |
| 5.12 | OMNeT++ simulation network of 5 nodes | 38 |
| 5.13 | LoRa P2P network simulation results, showing the number of sent new polygons per LoRa node with regards to the time, (a), (b) and (c) contain 2, 5 and 10 respectively. | 39 |
| 5.14 | Ditto for old / known polygons | 39 |
| 5.15 | LoRa P2P network simulation results, showing the number of received new generated polygons per LoRa node with regards to the time | 40 |
| 5.16 | Ditto for old / known polygons | 40 |
| 5.17 | Applied polygons of group 3 (Machine 1 and Machine 2), which are tracked by the server. Base map and data from OpenStreetMap and OpenStreetMap Foundation | 42 |
| 5.18 | OpenStreetMap representing known polygons of Machine 1, where the black polygons are the applied areas of Machine 1 and the blue polygons show the applied polygons of other participants of group 3 (Machine 2). Base map and data from OpenStreetMap and OpenStreetMap Foundation | 42 |

| | |
|--|----|
| 5.19 Ditto for Machine 2. Base map and data from OpenStreetMap and OpenStreetMap Foundation | 42 |
|--|----|

List of Tables

| | | |
|-----|---|----|
| 4.1 | Representation of group identifiers | 17 |
| 5.1 | Results of experiment 1, where LoRa was tested around a powerline towerFigure 5.2 | 34 |
| 5.2 | Results of experiments 2 to 4, where LoRa was tested in varying distances in a pine tree forest Figure 5.3 | 34 |
| 5.3 | Results of experiments 5 to 7, where LoRa was tested in different distances in the flat countryside of northern Germany Figure 5.4 . . . | 36 |
| 5.4 | Results of experiments 8 to 13, where LoRa was tested in different distances in the hilly countryside of Mid-Germany Figure 5.7/ Figure 5.6 | 36 |

Bibliography

- [1] D. Bochtis, S. Vougioukas, Y. Ampatzidis, and C. Tsatsarelis, “Field Operation Planning for Agricultural Vehicles: A Hierarchical Modeling Framework,” *PKP Publishing Services Network: Agricultural Engineering International: the CIGR Journal of Scientific Research and Development*, vol. IX, Feb. 2007.
- [2] L. Nóbrega, P. Gonçalves, P. Pedreira, and J. Pereira, “An IoT-Based Solution for Intelligent Farming,” *MDPI Sensors*, vol. 19, no. 3, 2019. DOI: 10.3390/s19030603.
- [3] N. Islam, M. M. Rashid, F. Pasandideh, B. Ray, S. Moore, and R. Kadel, “A Review of Applications and Communication Technologies for Internet of Things (IoT) and Unmanned Aerial Vehicle (UAV) Based Sustainable Smart Farming,” *MDPI: Sustainability*, vol. 13, no. 4, 2021. DOI: 10.3390/su13041821.
- [4] B. Wu, J. Meng, F. Zhang, X. Du, M. Zhang, and X. Chen, “Applying remote sensing in precision farming-a case study in Yucheng,” in *2010 World Automation Congress*, Kobe, Japan: IEEE, Sep. 2010.
- [5] F. Klingler, J. Blobel, and F. Dressler, “Agriculture meets IEEE 802.11p: A Feasibility Study,” in *2018 15th International Symposium on Wireless Communication Systems (ISWCS)*, Lisbon, Portugal: IEEE, Aug. 2018. DOI: 10.1109/ISWCS.2018.8491239.
- [6] O. Ali, B. S. Germain, J. Van Belle, P. Valckenaers, H. Van Brussel, and J. Van Noten, “Multi-Agent Coordination and Control System for Multi-Vehicle Agricultural Operations,” in *Proceedings of the 9th International Conference on Autonomous Agents and Multiagent Systems (AAMAS 10)*, vol. 1, Toronto, Canada: International Foundation for Autonomous Agents and Multiagent Systems, May 2010, pp. 1621–1622.
- [7] K. Karlsson, C. Bergenhem, and E. Hedin, “Field Measurements of IEEE 802.11p Communication in NLOS Environments for a Platooning Application,” in *2012 IEEE Vehicular Technology Conference (VTC Fall)*, Quebec City, QC, Canada: IEEE, Sep. 2012. DOI: 10.1109/VTCFall.2012.6399065.

- [8] C. Sommer and F. Dressler, Vehicular Networking. Cambridge University Press, Dec. 2014. DOI: 10.1017/CBO9781107110649.
- [9] D. Jiang and L. Delgrossi, “IEEE 802.11p: Towards an International Standard for Wireless Access in Vehicular Environments,” in *VTC Spring 2008 - IEEE Vehicular Technology Conference*, Marina Bay, Singapore: IEEE, May 2008, pp. 2036–2040. DOI: 10.1109/VETECS.2008.458.
- [10] “LTE-M Deployment Guide – Release 3,” GSMA, white paper 3, Jun. 2019, <https://www.gsma.com> -> Internet of Things -> Mobile IoT (LPWA) -> LTE-M -> LTE Deployment Guide.
- [11] M. Lauridsen, I. Z. Kovacs, P. Mogensen, M. Sorensen, and S. Holst, “Coverage and Capacity Analysis of LTE-M and NB-IoT in a Rural Area,” in *2016 IEEE 84th Vehicular Technology Conference (VTC-Fall)*, Montreal, QC, Canada: IEEE, Sep. 2016. DOI: 10.1109/VTCFall.2016.7880946.
- [12] “MOBILE IOT GUIDE HOW NB-IOT AND LTE-M ARE HELPING THE IOT TAKE OFF,” Deutsche Telekom AG, white paper 1.1, Feb. 2019, <https://iot.telekom.com> -> IoT -> NarrowBand IoT / LTE-M -> Mobile IoT Guide 2019.
- [13] O. Liberg, M. Sundberg, J. Bergman, Y.-P. E. Wang, and J. Sachs, Cellular Internet of Things: Technologies, Standards, and Performance. Academic Press (Elsevier), 2017. DOI: 10.1016/C2016-0-01868-5.
- [14] S. Dawaliby, A. Bradai, and Y. Poussset, “In depth performance evaluation of LTE-M for M2M communications,” in *2016 IEEE 12th International Conference on Wireless and Mobile Computing, Networking and Communications (WiMob)*, New York, NY, USA: IEEE, Oct. 2016. DOI: 10.1109/WiMOB.2016.7763264.
- [15] “Group Communication System Enablers (GCSE),” 3GPP, TS TS 22.468, version 17.0.1, 2020.
- [16] “On 5G mMTC requirement fulfilment, NB-IoT and eMTC connection density,” 3GPP, TDoc R1-1703865, 2017.
- [17] S. Bertoldo, L. Carosso, E. Marchetta, M. Paredes, and M. Allegretti, “Feasibility Analysis of a LoRa-Based WSN Using Public Transport,” *MDPI: Applied System Innovation*, vol. 1, no. 4, Dec. 2018. DOI: 10.3390/asi1040049.
- [18] A. Osorio, M. Calle, J. D. Soto, and J. E. Candeló-Becerra, “Routing in LoRaWAN: Overview and Challenges,” *IEEE Communications Magazine*, vol. 58, no. 6, pp. 72–76, Jun. 2020. DOI: 10.1109/MCOM.001.2000053.
- [19] J. P. Shanmuga Sundaram, W. Du, and Z. Zhao, “A Survey on LoRa Networking: Research Problems, Current Solutions, and Open Issues,” *IEEE Communications Surveys Tutorials*, vol. 22, no. 1, pp. 371–388, 2020. DOI: 10.1109/COMST.2019.2949598.

- [20] "Allgemeinzuteilung von Frequenzen zur Nutzung durch Funkanwendungen geringer Reichweite (SRD)," Bundesnetzagentur, Vfg. 133/2019, Dec. 2014, <https://www.bundesnetzagentur.de> -> Themengebiete -> Telekommunikation -> Frequenzen -> Allgemeinzuteilungen -> SRD.
- [21] A. H. Jebril, A. Sali, A. Ismail, and M. F. A. Rasid, "Overcoming Limitations of LoRa Physical Layer in Image Transmission," *MDPI Sensors*, vol. 18, no. 10, Sep. 2018. doi: 10.3390/s18103257.
- [22] J. C. Liando, A. Gamage, A. W. Tengourtius, and M. Li, "Known and Unknown Facts of LoRa: Experiences from a Large-scale Measurement Study," *ACM Transactions on Sensor Networks*, vol. 15, no. 2, Feb. 2019. doi: 10.1145/3293534.
- [23] N. E. Rachkidy, A. Guitton, and M. Kaneko, "Decoding Superposed LoRa Signals," in *2018 IEEE 43rd Conference on Local Computer Networks (LCN)*, Chicago, IL, USA: IEEE, Oct. 2018, pp. 184–190. doi: 10.1109/LCN.2018.8638253.
- [24] P. Robyns, P. Quax, W. Lamotte, and W. Thenaers, "A Multi-Channel Software Decoder for the LoRa Modulation Scheme," in *Proceedings of the 3rd International Conference on Internet of Things, Big Data and Security, IoT BDS 2018*, Funchal, Madeira, Portugal: SCITEPRESS – Science and Technology Publications, Mar. 2018, pp. 41–51. doi: 10.5220/0006668400410051.
- [25] M. Xhonneux, D. Bol, and J. Louveaux, "A Low-complexity Synchronization Scheme for LoRa End Nodes", Dec. 2019. arXiv: 1912.11344 [eess.SP].
- [26] J. Petajajarvi, M. Pettissalo, E. Marchetta, M. Paredes, and M. Allegretti, "On the Coverage of LPWANs: Range Evaluation and Channel Attenuation Model for LoRa Technology," Copenhagen, Denmark: IEEE, Dec. 2015, pp. 55–59. doi: 10.1109/ITST.2015.7377400.
- [27] M. Aref and A. Sikora, "Free space range measurements with Semtech Lora™ technology," in *2014 2nd International Symposium on Wireless Systems within the Conferences on Intelligent Data Acquisition and Advanced Computing Systems, Odessa, Ukraine*, Sep. 2014, pp. 19–23. doi: 10.1109/IDAACS-SWS.2014.6954616.
- [28] N. Gonzalez, A. Van Den Bossche, and T. Val, "Specificities of the LoRa™ Physical Layer for the Development of New Ad Hoc MAC Layers," in *17th International Conference on Ad Hoc Networks and Wireless, ADHOC-NOW 2018*, Saint-Malo, France: Springer International Publishing, Sep. 2018, pp. 163–174. doi: 10.1007/978-3-030-00247-3_16.

- [29] Y. Ji and H. Yang, “Comparation of LoRa and NB-IoT,” *CANADIAN CENTER OF SCIENCE AND EDUCATION: Network and Communication Technologies*, vol. 4, no. 1, pp. 13–16, Jun. 2019. DOI: 10.5539/nct.v4n1p13.
- [30] J. D. Luck, T. Stombaugh, and S. Shearer, “Basics of Automatic Section Control for Agricultural Sprayers,” *Agricultural Engineering*, no. 102, Jun. 2011, from Agriculture and Natural Resources program of University of Kentucky Cooperative Extension: <https://anr.ca.uky.edu/> -> ANR Publications -> Machinery and Equipment.
- [31] W. Ye, J. Heidemann, and D. Estrin, “An energy-efficient MAC protocol for wireless sensor networks,” in *Proceedings.Twenty-First Annual Joint Conference of the IEEE Computer and Communications Societies*, vol. 3, New York, NY, USA: IEEE, Jun. 2002, pp. 1567–1576. DOI: 10.1109/INFCOM.2002.1019408.
- [32] M. Derakhshani, Y. Khan, D. T. Nguyen, S. Parsaeefard, A. Dalili Shoaei, and T. Le-Ngoc, “Self-Organizing TDMA: A Distributed Contention-Resolution MAC Protocol,” *IEEE Access*, vol. 7, pp. 144 845–144 860, Sep. 2019. DOI: 10.1109/ACCESS.2019.2942114.
- [33] M. Lombardi, “Microsecond Accuracy at Multiple Sites: Is It Possible Without GPS?” *Instrumentation & Measurement Magazine, IEEE*, vol. 15, pp. 14–21, Oct. 2012. DOI: 10.1109/MIM.2012.6314510.
- [34] A. Vesa, F. Alexa, and H. Baltă, “Comparisons between 2D and 3D uniform array antennas,” in *2015 Federated Conference on Computer Science and Information Systems (FedCSIS)*, Lodz, Poland, Sep. 2015, pp. 1285–1290. DOI: 10.15439/2015F266.